

	Meteosat Second Generation	
VCS/DADF/UST/DSP/016 Issue: 5.0 Date: 1999-08-23	DADF User Station Design Justification	EUM/MSG/SPE/128 Issue: 5.0 Date: 1999-08-23

DADF Facility
DADF User Station Design Justification

	Meteosat Second Generation	
VCS/DADF/UST/DSP/016 Issue: 5.0 Date: 1999-08-23	DADF User Station Design Justification Document Signature Table	EUM/MSG/SPE/128 Issue: 5.0 Date: 1999-08-23

Document Signature Table

	Name	Function	Signature	Date
Author	Oliver Harrmann Sabine Nordmann Dr. Paul Crawford	Element Manager Software Engineer VCS Consultant		
Approval				
Approval				
Release	H. Wulf	Project Manager		
Eumetsat Approval				

	Meteosat Second Generation	
VCS/DADF/UST/DSP/016 Issue: 5.0 Date: 1999-08-23	DADF User Station Design Justification Document Change Record	EUM/MSG/SPE/128 Issue: 5.0 Date: 1999-08-23

Document Change Record

Issue/Revision	Date	DCN No.	Changed Pages/Paragraphs
1.0	24-Oct-97		Initial Release
1.1	18-Dec-97		Section 2 and 3 are changed
3.0	22-Jun-98		Sect. 3.1, 3.2, 4.1, 4.2, 4.3, 4.4 are changed
4.0	22-Jan-99		Change bars mark changes.
<u>5.0</u>	<u>1999-08-23</u>		<u>Change bars mark changes</u>

	Meteosat Second Generation	
VCS/DADF/UST/DSP/016 Issue: 5.0 Date: 1999-08-23	DADF User Station Design Justification Distribution List	EUM/MSG/SPE/128 Issue: 5.0 Date: 1999-08-23

Distribution List

Internal Distribution	
Name	No. Copies
VCS Archive, Dev	2

External Distribution		
Company	Name	No. Copies
EUMETSAT		4

	Meteosat Second Generation	
VCS/DADF/UST/DSP/016 Issue: 5.0 Date: 1999-08-23	DADF User Station Design Justification Table of Contents	EUM/MSG/SPE/128 Issue: 5.0 Date: 1999-08-23

Table of Contents

DOCUMENT SIGNATURE TABLE	I
DOCUMENT CHANGE RECORD	II
DISTRIBUTION LIST.....	III
TABLE OF CONTENTS	IV
LIST OF FIGURES	VI
LIST OF TABLES	VII
1 INTRODUCTION.....	1
1.1 PURPOSE AND SCOPE OF THE JUSTIFICATION	1
1.2 DOCUMENT STRUCTURE	1
1.3 OPEN ISSUES AND ASSUMPTIONS.....	2
1.4 APPLICABLE AND REFERENCE DOCUMENTS	2
1.4.1 Applicable Documents.....	2
1.4.2 Reference Documents.....	3
2 USER STATION CONTEXT	4
3 USER STATION ARCHITECTURE	6
3.1 HARDWARE ARCHITECTURE	6
3.1.1 Bespoke Hardware/Firmware Solution.....	6
3.1.2 PC Workstation	6
3.2 DEFINITION OF INTERNAL INTERFACES	7
3.3 SOFTWARE ARCHITECTURE.....	8
3.3.1 Selection of Operating System	8
3.3.1.1 Excellent Pedigree	8
3.3.1.2 Common DADF Operating System.....	8
3.3.1.3 Reduced System Management Costs	8
3.3.1.4 Support for TCP/IP	8
3.3.1.5 Client/Server versus Multi-User	8
3.3.1.6 Motif and Windows NT	9
3.3.1.7 Open Systems	9
3.3.2 User station functionality	9
4 RF FRONT-END	11
4.1 G/T CALCULATION.....	11
4.1.1 Antenna Gain.....	11
4.1.2 Loss Due to Pointing Error	12
4.1.3 System Noise Temperature.....	13
4.1.4 Spread Sheet Results.....	14
4.2 HRUS ANTENNA RESULTS	16
4.3 LRUS ANTENNA RESULTS	16
4.4 LOCAL OSCILLATOR PERFORMANCE	16
4.4.1 Choice of 1 st LO Frequency.....	16
4.4.2 Frequency Stability	16
4.4.3 Spectral Purity	17
4.5 REMOTE S-METER MONITORING FACILITIES	18
4.6 TEST SIGNAL INJECTION.....	19

	Meteosat Second Generation	
VCS/DADF/UST/DSP/016 Issue: 5.0 Date: 1999-08-23	DADF User Station Design Justification Table of Contents	EUM/MSG/SPE/128 Issue: 5.0 Date: 1999-08-23

5	MSG USER STATION BASEBAND MODULE	20
5.1	OVERALL ARCHITECTURAL APPROACH.....	20
5.2	DESIGN OF MUBM SIGNAL CONDITIONER.....	20
5.2.1	Overview.....	20
5.2.2	Design Parameters.....	21
5.2.3	Summary of Technology Loss Terms	24
5.2.4	Hardware Architecture.....	24
5.2.5	FIFO Buffer Requirements	24
5.2.6	Carrier Phase Error Algorithm	25
5.2.6.1	HRIT System	25
5.2.6.2	LRIT System	27
5.2.7	Bit Timing Error Algorithm	27
5.3	DESIGN OF THE DECODER.....	29
5.4	DESIGN OF THE PN GENERATOR.....	29
6	SOFTWARE.....	30
7	SIMULATORS AND TEST EQUIPMENT	31
7.1	USER STATION TEST HARNESS	31
7.2	MUBM TESTMODULATOR	31
7.2.1	Principles	31
7.2.2	Error Rate Determination	31
7.2.3	Eb/No Measurement	32
7.2.4	Analysis of Accuracy	34
8	GLOSSARIES.....	37
9	ANNEX A: USER STATION DATA DICTIONARY	38
10	ANNEX B: PLL DESIGN AND SIMULATION	39
11	ANNEX C: DESIGN OF BASEBAND PROCESSING	40
12	ANNEX D: HARRIS HSP50214 FILTER COEFFICIENT TABLE	41
13	ANNEX E: MATHCAD FILES	43

	Meteosat Second Generation	
VCS/DADF/UST/DSP/016 Issue: 5.0 Date: 1999-08-23	DADF User Station Design Justification List of Figures	EUM/MSG/SPE/128 Issue: 5.0 Date: 1999-08-23

List of Figures

Figure 1: US Software Architecture.....	10
Figure 2: LNA/downconverter Assembly Block Diagram	11
Figure 3: MUBM Signal Processing Block Diagram.....	24
Figure 4: DSP Software CPU Load Diagram	25
Figure 5: Direct Computation of QPSK Non-Linearity.....	26
Figure 6: Carrier and AGC Code Example.....	27
Figure 7: Bit Sync ZCD Timing Error Detector Code Example	28
Figure 8: Bit Sync Loop Filter Code Example	29
Figure 9: Theoretical E_b/N_0 curves.	35

	Meteosat Second Generation	
VCS/DADF/UST/DSP/016 Issue: 5.0 Date: 1999-08-23	DADF User Station Design Justification List of Tables	EUM/MSG/SPE/128 Issue: 5.0 Date: 1999-08-23

List of Tables

Table 1: LRUS and HRUS cost breakdown structure	5
Table 2: G/T Calculation	15
Table 3: 1 st Frequency Stability Budget.....	17
Table 4: 1 st Downconverter Oscillator Purity	18
Table 5: IF Frequency and Filter Design.....	21
Table 6: HSP50214 Configuration Parameters.....	22
Table 7: HRIT QPSK Loop Parameters	23
Table 8: LRIT BPSK Loop Parameters	23
Table 9: Bit Synchroniser Characteristics	23
Table 10: Technology Loss	24
Table 11: Error Analysis Budget.....	36

	Meteosat Second Generation	
VCS/DADF/UST/DSP/016 Issue: 5.0 Date: 1999-08-23	DADF User Station Design Justification Introduction	EUM/MSG/SPE/128 Issue: 5.0 Date: 1999-08-23

1 Introduction

1.1 Purpose and Scope of the Justification

This document provides a justification for the User Station design. Great care is taken for the justification of the dedicated hard- and firmware development to the challenging requirements in the area of the RF Front-End and the digital demodulation and baseband processing. For this two technical notes are appended in the annex of this document. The main aspects are covered directly in the body of this document. In addition the physical implementation of the bespoke hardware/firmware and COTS hardware of the User Station are discussed.

The justification for the software design is also reflected in this document but here no serious difficulties are mentioned through the whole architectural design phase.

1.2 Document Structure

The document structure is according to the main sections of the [USDS] document. The [FDS] standard is taken into account but several sections are left out due to the non-conformance to the special User Station aspects.

Section Title	Description
Introduction	This is the introduction of the document.
User Station Context	This section gives a justification for the US context as seen by VCS.
User Station Architecture	This section gives a justification for the top-level architectural design w.r.r the split of COTS hardware and software and bespoke hardware/firmware. The PC workstation hardware is discussed.
RF Front-End	This section gives a justification for the design of the RF Front-End.
MSG User Station Baseband Module	This section gives a summary justification for the design of the MUBM w.r.t. theoretical and implementation aspects. Further justification is found in the annexed technical notes.
Software	This section gives a justification for the shows a decomposition of all software components and specifies the architecture of the software.
Simulators and Test Equipment	This section gives a justification of the test tools
Glossaries	This section refers to the common DADF glossary
Annex A: User Station Data Dictionary	This section refers to the common DADF data dictionary, which is a self-standing document.
Annex B: PLL Design and Simulation	This section contains a technical note, which is the justification for the PLL design
Annex C: Baseband Processing	This section contains a technical note, which ii the justification for the baseband processing design
Annex D: Harris HSP50214 Filter coefficients	This section contains the caculated filter coefficients for the detailed design
Annex E: Mathcad files	This section contains the mathcad files used to perform the theoretical calculations provided in the main

	Meteosat Second Generation	
VCS/DADF/UST/DSP/016 Issue: 5.0 Date: 1999-08-23	DADF User Station Design Justification Introduction	EUM/MSG/SPE/128 Issue: 5.0 Date: 1999-08-23

Section Title	Description
	document.

For the following sections, no justification is meaningful, although included in the [USDS].

Section Title	Justification
Interfaces	The [USDS] only includes a summary.
Communications Network Architecture	This section is meaningless in the US context. It appears in the [USDS] context only for compliance with the [FDS]
Facility Common Standards	This section is meaningless in the US context. It appears in the [USDS] context only for compliance with the [FDS]
Requirements Trace	The [USDS] only includes a summary.
TBCs and TBDs	The [USDS] only includes a summary.

1.3 Open Issues and Assumptions

~~There are no open issues and assumptions. The most important issue is still the verification of the low technology loss of the MUBM for HRIT and LRIT case. This will be verified with the MUBM Testmodulator especially designed for simulating the LRIT/HRIT link including noise and EDA effects similar to the satellite downlink.~~

~~With regard to the detailed design, there are no open issues for the architecture of the system.~~

1.4 Applicable and Reference Documents

1.4.1 Applicable Documents

Acronym	Title	Reference
MSI	LRIT/HRIT Mission Specific Implementation	EUM/MSG/SPE/057
FDS	EUMETSAT Facility Development Standard	EUM/STD/FDS
SGICD	MSG Satellites to Ground Segment ICD	EUM/MSG/ICD/006
FRS	MSG GS DADF Requirement Specification	EUM/MSG/SPE/041
FGLO	VCS DADF Glossary	EUM/MSG/TEN/247TBD
FSDS-A	DADF Design Specification-Appendix A Data Dictionary,	TBD
FSDS	DADF Design Specification	EUM/MSG/SPE/112
USDJ	DADF User Stations Design Justification	EUM/MSG/SPE/128
FPSMU	Prototype specification for MUBM	EUM/MSG/SPE/113
FPER MUBM	Prototype Evaluation Report for MUBM	EUM/MSG/RPT/112TBD
FIICD	Facility Internal Interface Control Document User Station::	EUM/MSG/ICD/096TBD
US::DISE	Dissemination Element	
FUM SKU	User Manual Station Key Unit	TBD
FUM MUBM	User Manual MSG User Station Baseband Module	TBD
FUM DC	User Manual Downconverter	TBD

 VES ENGINEERING	Meteosat Second Generation	 EUMETSAT
VCS/DADF/UST/DSP/016 Issue: 5.0 Date: 1999-08-23	DADF User Station Design Justification Introduction	EUM/MSG/SPE/128 Issue: 5.0 Date: 1999-08-23

1.4.2 Reference Documents

Acronym	Title	Reference
FDS	EUMETSAT Facility Development Standard	EUM/STD/FDS
L/HRITGS	EUMETSAT LRIT/HRIT Global Specification, Rev.2.3	
MSA	Modern Structured Analysis, E. Yourdon, Prentice Hall, 1989, ISBN 0-13-598632	
UGSAF	User Guide, The System Architect Family of Tools, Popkin Software & Systems, part Number 1808-1.	
USDS	DADF User Station Design Specification	EUM/MSG/SPE/127
FSDS	DADF Design Specification	EUM/MSG/SPE/112
FDJ	DADF Design Justification	EUM/MSG/SPE/117
	EUMETSAT LRIT/HRIT Global Specification, Rev.2.3	
UGSAF	User Guide, The System Architect Family of Tools, Popkin Software & Systems, part Number 1808-1.	
SCSI	Small Computer System Interface – 2, ANSI X3T9.2/86-109 Rev.6	
RS422	EIA RS-422 TBD	
RS232	EIA RS-232 C TBD	

 VES ENGINEERING	Meteosat Second Generation DADF User Station Design Justification User Station Context	 EUMETSAT
VCS/DADF/UST/DSP/016 Issue: 5.0 Date: 1999-08-23		EUM/MSG/SPE/128 Issue: 5.0 Date: 1999-08-23

2 User Station Context

The basic idea is to have separate functions for LRIT and HRIT data processing. This is anyway required for dedicated hardware items such as RF-Front-End and the MUBM. The same approach is used for the other functions and the architectural design concerning hardware of the computers and software.

We could say that the DADF User Station is sub-divided into two systems, the LRIT User Station and the HRIT User Station System, LRUS and HRUS. This might be an advantage as each chain can be individually configured for DADF.

The Station Key Unit plays a special role in the User Station context. Although the device will be integrated in the MUBM enclosure, the interface is regarded to be an external one. This is due to the fact that also other User Station supplier shall be able to interface the SKU on base of standard interfaces. The definition of this interface will be covered under the DADF Key Centre Element design.

The interface to the DISE in DADF is also regarded to be an external. This interface plays only a special role in the DADF context. For standalone User Stations it is of no interest. On the other hand it can be used for dispatch purposes for MSG users to distribute MSG data.

The following tables give a cost breakdown structure for HRUS and LRUS stations. The MUBM costs are estimated on our experience from the US production phase, where the components have been built for the first time. Due to the fact that parts costs and manufacturing costs highly depends on the number of produced modules, this calculation can only give a first estimation. Approximately 20 to 30% of the given values are manufacturing costs.

The cost breakdown of the complete stations shows additional licence costs for the US application software. Again this highly depends on the policy the individual company selling these products. Therefore it is just estimation.

It shall be noted that minimising the design costs has driven the design of the MUBM, i.e. MUBMs for LRIT and HRIT are nearly the same (different firmware on the baseband processing side and the 2nd DC is adjusted slightly different). Furthermore there are ideas to reduce the MUBM hardware to one DSP processor by shifting the decoding functionality to the software, which reduces the price for 800 ECU.

A design minimising the re-production costs is beyond the scope of this project. Therefore the costs for the MUBM more or less reflects the re-production costs of the MUBM prototype.

LRIT / HRIT / MUBM	
Component	Estimated price (EURO/ECU)
1960-PB1 & 1960-PB2	850
1960-DSP X 2	3200
1960-DSPBPM	550
1960-GPI	450
1960-DISP	550
1960-2ndDC	1250
MUBM/FRM	1700
Total price	8550

LRIT User Station	
Component	Estimated price (EURO/ECU)

 VES ENGINEERING	Meteosat Second Generation DADF User Station Design Justification User Station Context	 EUMETSAT
VCS/DADF/UST/DSP/016 Issue: 5.0 Date: 1999-08-23		EUM/MSG/SPE/128 Issue: 5.0 Date: 1999-08-23

Antenna, 1.8 m, Andrew Model P6F-17C including mount	3200
1 st Downconverter	4900
LRIT MUBM	8550
PC Workstation	2300
19" Monitor	800
- Application Software – Real-time Data Reception, M&C User Station, Quick-look, Dispatch	4900
Total price	24650

HRIT User Station	
Component	Estimated price (EURO/ECU)
Antenna, 3.7 m, Andrew Model P12-17C including mount	7900
1 st Downconverter	4900
HRIT MUBM	8550
PC Workstation	3800
19" Monitor	800
- Application Software – Real-time Data Reception, M&C User Station, Quick-look, Dispatch	4900
Total price	30850

Table 1: LRUS and HRUS cost breakdown structure

It should be noted that these are price estimations and not guaranteed prices. It is assumed that the PC workstation for the HRUS system will need more disk capacity. This results in a higher price. The main difference between LRUS and HRUS are actually seen in the antenna costs.

The MUBM design under the DADF contract does not foresee a differentiation between the hardware modules in order to reduce the firmware design effort. This results in an identical price for HRIT and LRIT MUBM systems.

	Meteosat Second Generation	
VCS/DADF/UST/DSP/016 Issue: 5.0 Date: 1999-08-23	DADF User Station Design Justification User Station Architecture	EUM/MSG/SPE/128 Issue: 5.0 Date: 1999-08-23

3 User Station Architecture

3.1 Hardware Architecture

3.1.1 Bespoke Hardware/Firmware Solution

On one hand the User Station architecture is driven by the requirements of the [FRS]. In addition the prototyping activities in the area of the signal processing, i.e. the PLL design and simulations, the design of the baseband processing and the evaluation of different VLSI chips described within this document and the [FPER MUBM] are taken into account.

All this leads to the decomposition and detailed modelling shown in the [USDS]. In this section only a summary of the results should be given. The real justification for this design is given later. This order is forced by the order of the document, which gives a top down approach. The area of defining the border between hardware/firmware solution and the software, that runs on a PC workstation, is more justified by a bottom up design. First we have to see what is realistic only in hardware/firmware and then to identify the borderline.

Our approach is to perform nearly all performance intensive tasks in dedicated hardware/firmware due to following reasons:

- The actual performance of PC workstations is not sufficient to perform baseband processing, Viterbi decoding, RS decoding, triple DES PN pattern generation, decompression and in addition the operating system tasks including MMI support.
- The user shall have sufficient performance available for interactive tasks such as MMIs and other.

Taking our results into account, the borderline between hardware/firmware and software as shown in the [USDS] is as follows:

- The processing of the LRIT/HRIT protocol is done up to the VCDU assembly. This includes all baseband processing and the performance intensive task of RS decoding. A rough estimation of the performance figures for RS decoding leads to 50 to 100 MIPS for the HRIT case. It should be noted that other interfaces are reasonable. We could easily implement the source packet assembler or even the file assembler in firmware. One option could be the implementation of three different buffers in the MUBM. One buffering the VCDUs, the second buffering the source packets and the third buffering the XRIT (LRIT, HRIT) files. All of them are filled up in parallel. Different command sets would allow accessing one or the other buffer depending on the current US mode, which can be the VCDU trace, source packet trace or file assembly mode. The three-buffer option could be realised to reduce the workstation software complexity for packet and file assembly.
- The design approach for the PN generator has been changed during early DD phase due to the results of a prototype DES implementation running on an Intel platform, indicating that a PC having a second CPU will cope with the PN generation in real-time.
- It is required to include the SKU in the MUBM device. In order to have only one interface (SCSI-2) between MUBM and PC workstation, the foreseen serial interface of the SKU is not directly connected to the PC, although it would be possible and acceptable to have a direct interface between PC and SKU.
- The rationale to implement the decompression, as a performance intensive task, on the PC in software is mostly driven by the flexibility to add, remove or change decompression algorithms through out the lifetime of the MSG programme.

3.1.2 PC Workstation

The hardware architecture is mostly driven by the requirements. One open point has been the selection of the PC workstation hardware. The proposed configuration is shown in the [USDS]. The selection of the PC supplier is not of such importance. Here several solutions could also be possible.

	Meteosat Second Generation	
VCS/DADF/UST/DSP/016 Issue: 5.0 Date: 1999-08-23	DADF User Station Design Justification User Station Architecture	EUM/MSG/SPE/128 Issue: 5.0 Date: 1999-08-23

Disk Performance HRIT

The net data rate of the HRIT channel is 1 Mbit/sec. This results in a data rate of 125 E3 byte/sec. Assuming that all files are encrypted and compressed (worst case assumption) and the average compression factor is 3.5, the total data rate is $5.5 \times 125 \text{ E3 byte/sec} = 687.5 \text{ E3 byte/sec}$.

The file rate can be assumed by about 1.4 files/sec, which results in 4.2 files/sec.

This estimation only describes the main writing disk operations and does not include extra data for sub-sampled images or read operations caused by MMI access etc.

Disk Capacity HRIT

Taking into account the above-mentioned values, the total capacity for one-hour HRIT data is about 2.4 GB.

Solution

Taking into account the above-mentioned results, the selection of the disk drives is as follows:

- 1st Drive – 2 Gbytes for operating system and programmes
- 2nd Drive – 4 Gbytes for online storage
- 3rd Drive – 4 Gbytes for offline storage

In principle the capacity should be available on nearly one disk alone. The rationale is performance aspect w.r.t. data and file I/O. The system disk will be used frequently for system operations swap space etc.

Also the online disk storing all XRIT files at different processing stages and the sub-sampled image data is used frequently. Here additional access speed is useful for the quick look MMIs.

The offline storage is not of that importance although also high data rates could be possible when the multi-entry filter is configured to store all XRIT files in all processing stages on that disk.

Using one common disk for all these tasks would have a big negative impact on the overall performance of the User Station computers. No difference is made for the LRIT and the HRIT case. This is done to make all stations interchangeable.

3.2 Definition of Internal Interfaces

Two internal interfaces are identified in the [USDS]. The interface between Downconverter and MUBM, the IF interface, and the interface between MUBM and COTS PC.

The first one is more a commonly used interface based on the design heritage for MDD, PDUS and SDUS systems. There is no reason for changing the basic system, however, we have added a LF data system to support the remote S-meter with monitoring information such as signal strength, bit errorrate and other. This has been designed to maintain “reverse compatibility” with previous downconverters.

The second interface is an 8 bit single ended SCSI-2 interface [SCSI]. Here VCS has several firmware and hardware modules available. The usage of this interface leads to a reduction of design risks and a reduction in effort for the MUBM interface driver development. Due to the data rates calculated above, the performance of the SCSI-2 interface standard is sufficient.

The SCSI interface of the VCS system is compatible to the [SCSI] standard. The system is currently working together with a variety of different PC types including a variety of different SCSI PCI cards of single-ended wide SCSI and narrow SCSI type.

	Meteosat Second Generation	
VCS/DADF/UST/DSP/016 Issue: 5.0 Date: 1999-08-23	DADF User Station Design Justification User Station Architecture	EUM/MSG/SPE/128 Issue: 5.0 Date: 1999-08-23

3.3 Software Architecture

3.3.1 Selection of Operating System

Windows NT has been selected as the Operating System for the VCS DADF proposal. The discussion in this section provides a justification for this selection and, in particular, focuses on points, which may be of concern to EUMETSAT.

Additional EUMETSAT comment: It is recognised that the use of WINDOWS NT as Operating System for the US has so far (in the framework of integration and system testing) not revealed any particular problems, and there are also no indications for future ones. However, in the light of the recent decision of COMPAQ/Microsoft to stop the further development/support of WINDOWS NT for "Alpha" CPU based systems, there is some doubt about the long term reliability of Microsoft's policy regarding Operating Systems. This may have an impact on the validity of the discussion in the following sub-sections. It is not intended to reopen this discussion, particularly because the US Workstation is based on PCs with INTEL CPUs, and, as already said above, because no actual problems with WINDOWS NT in the framework of the User Stations have been encountered nor are expected. But, as general, overall valid statements, EUMETSAT would not fully support the view presented in the following sub-sections.

3.3.1.1 Excellent Pedigree

Windows NT draws its heritage from the well respected (but now dated) VMS Operating System. Many of the senior Windows NT development engineers, including the project manager, were members of the original VMS development team. VMS is well known for its robustness and, in particular it's real-time scheduling capabilities. NT has maintained this heritage and in addition as included some of the best ideas from industry, such as kernel level multi-threading; a robust new file system, NTFS, which supports file recovery, security features, and fault tolerance through redundancy; and symmetric multiprocessing (an important consideration for DADF in order to exploit the parallelism of the various compression algorithms).

3.3.1.2 Common DADF Operating System

EUMETSAT have mandated that the OFO and OFV environments are to be supported by PC based clients, hence Windows NT is necessarily to be employed in, at minimum, in these environments. The attendant advantages of employing a common Operating System throughout the DADF are apparent in terms of ease of integration and subsequent system management.

3.3.1.3 Reduced System Management Costs

It is well known that system management of Unix platforms is a complex and expensive procedure due to the need to 'hand edit' a number of obscure files scattered throughout the file system. In this sense, Unix reflects its historical pedigree from the 1970's.

Windows NT have simplified this by providing a full suite of GUI based tools for system management and monitoring. All system configuration information is centralised in a Registry which itself is accessible via a standardised GUI. The GUI based tools limit the range of configuration selections to a prescribed set of options; the possibilities for miss-configuration are thereby limited.

3.3.1.4 Support for TCP/IP

VCS has direct and positive experience with the use of the WinSock interface, a de facto standard, for Windows-based network programming. WinSock 1.1 was developed by a group of 30 vendors, including Microsoft. More recently WinSock 2.0 has been extended to include support for other communication protocols.

VCS routinely acquires the latest documentation concerning updates to the WinSock documentation via the 'Microsoft Development Network' and monthly updates to the Microsoft TechNet CD distribution network.

3.3.1.5 Client/Server versus Multi-User

To those familiar with host-based Operating Systems such as VMS or Unix, NT's lack of a multi-user capability

	Meteosat Second Generation	
VCS/DADF/UST/DSP/016 Issue: 5.0 Date: 1999-08-23	DADF User Station Design Justification User Station Architecture	EUM/MSG/SPE/128 Issue: 5.0 Date: 1999-08-23

comes as somewhat of a surprise. This reflects NT's adherence to the client/server model throughout its design and implementation (even the standard NT system services API, Win32, is only a client to a lower level kernel). Under NT, monitoring and control of remote systems is achieved via the use of client GUI based tools. Standard GUI based tools which are bundled with NT include the following:

- A Registry MMI for querying / editing the configuration of a local or remote system,
- A System Monitoring MMI for detailed monitoring of both the local machine and/or a remote machine (indeed this tool allows simultaneous real-time monitoring of system performance of more than one platform).
- A process / thread view MMI which allows real time monitoring and control of both local and remote processes.
- An Event MMI which allows interrogation of an event log on either the local or remote machine.

3.3.1.6 Motif and Windows NT

VCS undertook a detailed comparison of the 'OSF/Motif Style Guide' and the Windows equivalent, namely 'The Windows Interface Guidelines for Software Design' in order to ensure that Windows could be tailored to comply with the MSG Ground Segment Design Specification, Appendix A, and the DADF FMRS. Without exception it was found that the Windows environment either directly provides the features mandated by EUMETSAT or can be tailored to do so. Indeed this conclusion is not surprising given that this interface is ubiquitous in industry and is therefore supported by GUI builders who support both the building of specific MMI screens and the building of individual components, which can then be re-used.

3.3.1.7 Open Systems

The phrase Open Systems has many different interpretations, nevertheless, the goal of Open Systems is the same regardless of the definition of the term. Its primary aim is to give a user cost-effective choices in a multi-vendor world that is in a constant state of change. There are two categories of standards: *de jure* and *de facto*, the former referring to formal standards created by standards bodies. A good example of this is the IEEE Portable Operating System Interface for Unix (POSIX). De facto standards are those that are widely adopted by industry, but were not originally endorsed by any of the standards bodies (a good example of such a standard is the Transmission Control Protocol / Internet Protocol (TCP/IP)).

The inevitable problem with de jure standards is that, in general, they are not able to keep pace with the rapid development of technology, and hence de facto standards tend to arise to fulfil an industrial need.

Windows NT has addressed the conflict between *de jure* and *de facto* standards by providing support for two system services API's, namely the POSIX standard, previously mentioned and its own elegant system services API, Win32. Microsoft were able to do this by defining the system services API to itself be simply a client to a lower level kernel server, which meant that more than 1 system services API (client) is supported. Unix software can be ported to NT if it conforms to the POSIX standard.

3.3.2 User station functionality

After the decision about the interface between the MUBM and Workstation software, the following functionality shall implemented by the software:

A reception process works permanently to read VCDUs available in the MUBM, assemble them to LRIT/HRIT files and pass the files to a process which store them to a disk location called online buffer.

This online buffer is administrated and controlled by a process, which analyse the received file, decide the further processing and store all created versions of the LRIT/HRIT file. After internal processing is completed, data are provided for the transfer to the DISE-element in a DADF-environment. Each LRIT/HRIT has assigned a lifetime, after that is passed the file and all its versions will be deleted.

	Meteosat Second Generation	
VCS/DADF/UST/DSP/016 Issue: 5.0 Date: 1999-08-23	DADF User Station Design Justification User Station Architecture	EUM/MSG/SPE/128 Issue: 5.0 Date: 1999-08-23

To retain data stored in the online buffer longer than their lifetime, extra offline areas are specified. Data can be transferred from online to these offline areas.

The contents of each buffer may be displayed by a set of viewer contained in the MMIs. The offline areas completely controlled by the user via the MMIs.

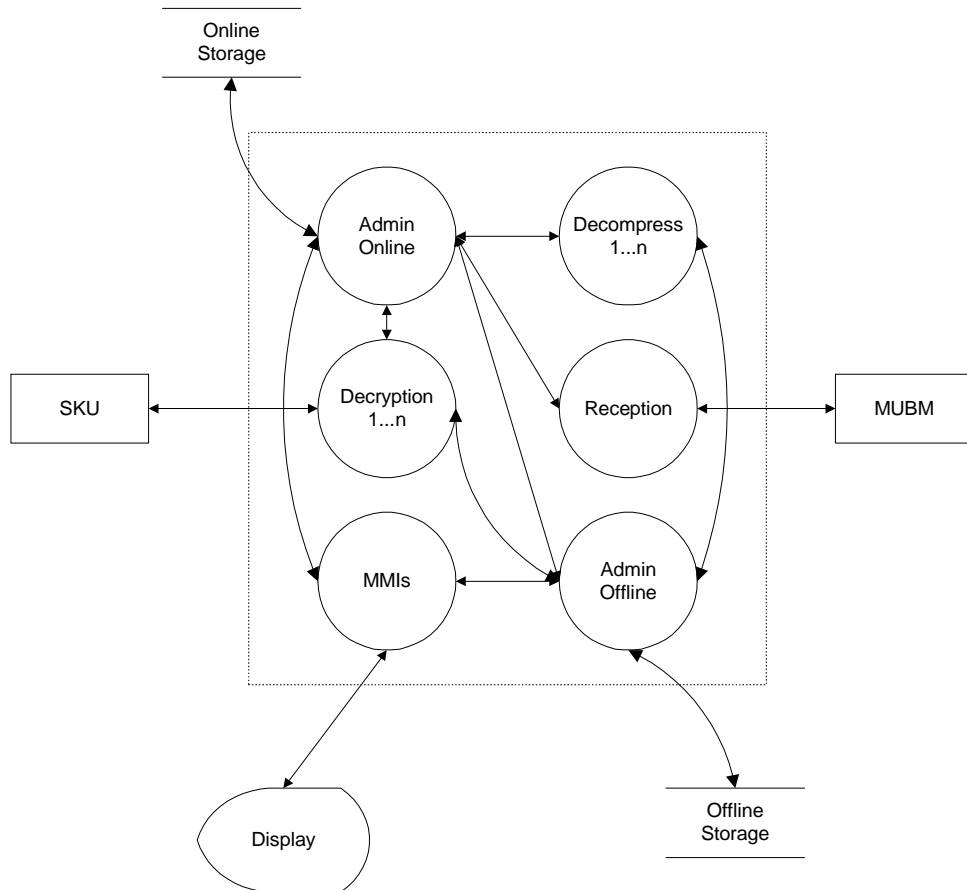


Figure 1: US Software Architecture

 VES ENGINEERING	Meteosat Second Generation DADF User Station Design Justification RF Front-End	 EUMETSAT
VCS/DADF/UST/DSP/016 Issue: 5.0 Date: 1999-08-23		EUM/MSG/SPE/128 Issue: 5.0 Date: 1999-08-23

4 RF Front-End

The RF Front-End consists of both the Antenna/feed assembly, and the LNA/downconverter assembly. The block diagram of the LNA/downconverter is shown in Figure 2 below and the detailed specifications can be found in the corresponding Front-End DD document.

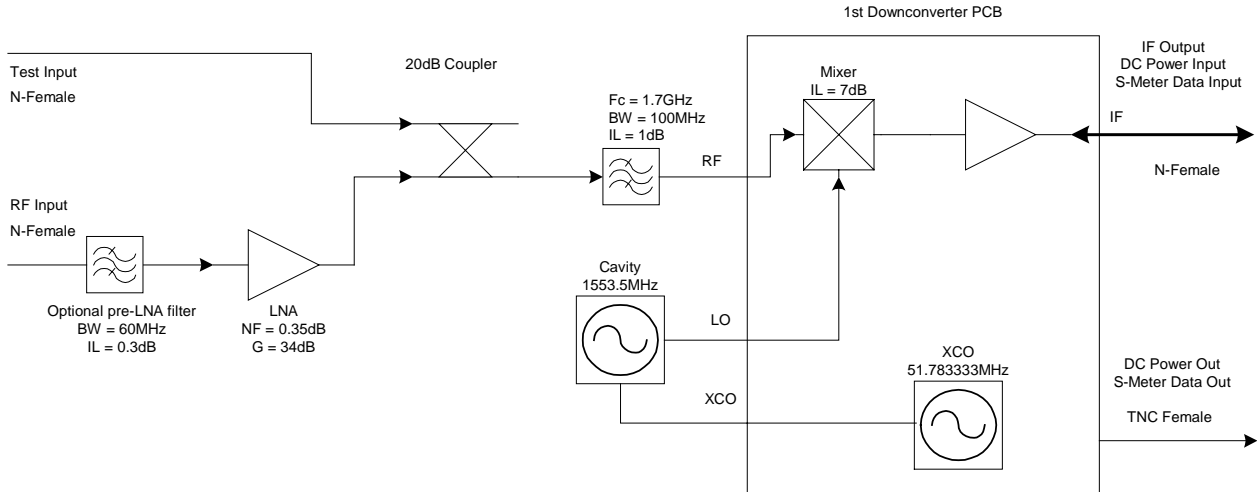


Figure 2: LNA/downconverter Assembly Block Diagram

Justifications of the choice of Antenna/feed, together with the LNA/downconverter performance, are covered in the following sections.

4.1 G/T Calculation

4.1.1 Antenna Gain

The basic values for gain and size are obtained from the Andrew catalogue and the resulting values computed using the approximation of the ideal uniformly illuminated circular aperture.

For a uniformly illuminated circular aperture the directivity gain is given (Balanis, C. A., 1997, p607, eqn 12-56) by:

$$G = \frac{4\pi}{\lambda^2} \text{area} \quad 1$$

Where λ is the wavelength ($\lambda = c/f = 0.177\text{m}$, with $c=299.792458 \times 10^6 \text{ ms}^{-1}$ and f in MHz) and the area is πr^2 , the radius r taken as half of the catalogue diameter D , hence:

$$G = \frac{4\pi}{\lambda^2} \pi \left(\frac{D}{2} \right)^2 = \left(\frac{\pi D}{\lambda} \right)^2 \quad 2$$

In the real case, the gain is less than this ideal due to both small ohmic losses in the feed and the non-uniform illumination of the aperture (the parabolic reflector in this case). Such illumination profile is necessary due to the finite extent of the feed and to control sidelobe and backlobe levels. To account for the illumination pattern, the concept of illumination efficiency can be used, this is the directivity gain achieved relative to the ideal case. Modifying the above formula we have:

$$G = \frac{\eta}{100} \left(\frac{\pi D}{\lambda} \right)^2 \quad 3$$

 VCS ENGINEERING	Meteosat Second Generation DADF User Station Design Justification RF Front-End	 EUMETSAT
VCS/DADF/UST/DSP/016 Issue: 5.0 Date: 1999-08-23		EUM/MSG/SPE/128 Issue: 5.0 Date: 1999-08-23

Where the efficiency η is expressed in percent. To find this value, we adjusted η until the gain obtained was the same as the published values from the Andrew catalogue. This is likely to be pessimistic since they have already accounted for the ohmic losses as well.

For a uniformly illuminated circular aperture, the beamwidth (angle between the two -3dB points in any specified plane) is given (Balanis, C. A., 1997, p609, noting that $a=D/2$) by:

$$\theta_{3dB} = \frac{58.4\lambda}{D} \quad 4$$

where the angle is expressed in degrees. By rearranging equation 2 we have:

$$\frac{\lambda}{D} = \frac{\pi}{\sqrt{G}} \quad 5$$

Hence the beamwidth for the non-ideal illumination case can be estimated from:

$$\theta_{3dB} \approx \frac{58.4\pi}{\sqrt{G}} \approx \frac{183.5}{\sqrt{G}} \quad 6$$

4.1.2 Loss Due to Pointing Error

To estimate the loss due to pointing errors we need to know the beam error and the effect of this on the antenna directivity.

If we have two points (X and Y) specified by azimuth A and elevation E (or the equivalent of Right Ascension and Declination for celestial co-ordinates) in radians, we can compute the pointing angle P between them from spherical trigonometry (Green, 1985, p12, eqn 1.11):

$$\cos(P) = \sin(E_X)\sin(E_Y) + \cos(E_X)\cos(E_Y)\cos(A_X - A_Y) \quad 7$$

Noting the power series for the cosine function is:

$$\cos(x) = 1 - \frac{x^2}{2!} + \frac{x^4}{4!} - \dots \quad 8$$

It is clear that care should be used in the computation since the effect of finite precision (about 1.2E-7 for IEEE single precision 2.2E-16 for double precision) on the $\cos(P)$ term is such that P is only determined to about $\sqrt{2! \cdot 2\epsilon} \approx 3 \cdot 10^{-8}$ radian (around 1.7E-6°) in double precision and only 0.04° in the single precision case.

This calculation is usually approximated by:

$$P \approx \sqrt{(E_X - E_Y)^2 + [(A_X - A_Y)\cos(E_X)]^2} \quad 9$$

when the angles are very small, for example if $\cos(P) > 0.999999$, which implies that E_X and E_Y are almost identical so the choice of elevation used, $\cos(E_X)$, is not important.

If we are looking at the spacecraft close to the equator, and we do not require very high accuracy, then it is acceptable to calculate the spacecraft movement as:

$$P \approx \sqrt{\Delta L^2 + \Delta I^2} \quad 10$$

 VCS ENGINEERING	Meteosat Second Generation	 EUMETSAT
VCS/DADF/UST/DSP/016 Issue: 5.0 Date: 1999-08-23	DADF User Station Design Justification RF Front-End	EUM/MSG/SPE/128 Issue: 5.0 Date: 1999-08-23

Where ΔL is the shift in longitude (0.5°) and ΔI is the shift due to inclination (1.0°) resulting in a total shift of 1.12° about the nominal centre location (from US.230). Since manual adjustment errors could occur in any direction, the worst case combination is the sum of this with the manual error.

To compute the pointing error loss, the usual method is to approximate the antenna directivity pattern as a quadratic equation since any smooth function with a maxima or minima has a zero 1st derivative at that point, hence the Taylor series about that point will have the constant, 2nd power term and higher terms only. Close to the expansion point for the series only the 2nd power term will be significant and the simplest option is to ignore higher order terms if an approximation is not known or required.

A simple formula which expresses this as a quadratic in $\log(\text{Power})$ is:

$$\Delta G \approx 12 \left(\frac{\theta}{\theta_{3dB}} \right)^2 \quad 11$$

since $\log(1+x)$ is approximately x for $x \ll 1$. Here ΔG is the loss in dB from a pointing error θ in degrees (if θ_{3dB} is measured in degrees). Clearly the value of $\theta = 0.5 * \theta_{3dB}$ should result in a loss of 3dB. This formula is very close to the ideal illuminated aperture down to 5dB or so, beyond this it fails to show the zeros in the radiation pattern, but that is not important here.

This allows the G in G/T to be computed. For the T we need to account for the sky noise and the ohmic losses prior to the LNA/Downconverter assembly.

4.1.3 System Noise Temperature

The sky noise is the most difficult term to obtain, sometimes this is quoted by the antenna manufacturer but it depends upon the sky temperature profile (available from standard literature, except for any local effects such as tall trees, hills and buildings) and the antenna radiation pattern (in particular, the sidelobe and backlobe contributions).

To account for the losses (the feed and any pre-LNA filter) we assume they are at the same temperature, so the effective noise factor of the attenuation is:

$$F_{LOSS} = 1 + \frac{T_A}{T_O} (L - 1) \quad 12$$

Where T_A is the attenuator physical temperature in Kelvin, T_O is 290K (used in the definition of noise factor/figure) and L is the total loss (1/Gain) before the LNA/Downconverter, expressed as a numerical ratio.

The noise temperature for the whole system is the sum for the sky noise temperature and the effect of the electronics. For the cascade of the pre-LNA attenuation and the LNA/Downconverter, the noise factor is:

$$F_{EQ} = F_1 + \frac{F_2 - 1}{G_1} + \frac{F_3 - 1}{G_1 G_2} + \dots + \frac{F_N - 1}{G_1 G_2 \dots G_{N-1}} \quad 13$$

Or in noise temperatures:

$$T_{EQ} = T_1 + \frac{T_2}{G_1} + \frac{T_3}{G_1 G_2} + \dots + \frac{T_N}{G_1 G_2 \dots G_{N-1}} \quad 14$$

The conversion from noise factor to temperature is given by:

$$T_{EQ} = T_O (F - 1) \quad 15$$

and inversely by:

 VCS ENGINEERING	Meteosat Second Generation DADF User Station Design Justification RF Front-End	 EUMETSAT
VCS/DADF/UST/DSP/016 Issue: 5.0 Date: 1999-08-23		EUM/MSG/SPE/128 Issue: 5.0 Date: 1999-08-23

$$F = 1 + \frac{T_{EQ}}{T_O} \quad 16$$

Hence the total system noise temperature T_{SYS} is given by:

$$T_{SYS} = T_{ANT} + T_{RX} = T_{ANT} + T_O(F_{RX} - 1) \quad 17$$

Where the equivalent receiver noise factor F_{RX} is given by:

$$F_{RX} = F_{LOSS} + \frac{(F_{LNA} - 1)}{G_{LOSS}} \quad 18$$

based on eqn 12 and eqn 13, and assuming F_{LNA} includes the post-LNA (downconverter and receiver) noise contributions.

Since $L = 1/G_{LOSS}$ this leads to:

$$T_{SYS} = T_{ANT} + T_O((F_{LOSS} + L(F_{LNA} - 1)) - 1) \quad 19$$

as the overall system noise temperature. The "figure of merit" G/T is then simply G_{ANT}/T_{SYS} and is usually expressed in dBK^{-1} .

4.1.4 Spread Sheet Results

The calculation of the G/T for the MSG system is performed by a spreadsheet and is included here. The spreadsheet is arranged as 8 columns with identical calculations for each of the cases. These are:

- LRUS, and HRUS.
- Nominal and Worst case.
- Without pre-LNA filter, and with optional design fitted.

 VES ENGINEERING	Meteosat Second Generation DADF User Station Design Justification RF Front-End	 EUMETSAT
VCS/DADF/UST/DSP/016 Issue: 5.0 Date: 1999-08-23		EUM/MSG/SPE/128 Issue: 5.0 Date: 1999-08-23

Parameter	Units	Without pre-LNA Filter				With pre-LNA Filter			
		LRUS	LRUS	HRUS	HRUS	LRUS	LRUS	HRUS	HRUS
System		Nominal	Worst	Nominal	Worst	Nominal	Worst	Nominal	Worst
Target G/T	dB/K	6	5	14	12	6	5	14	12
Frequency	MHz	1691	1691	1695.15	1695.15	1691	1691	1695.15	1695.15
Maximum satellite movement (inclination and longitude)	degree	0	0	0	0	0	0	0	0
Manual adjustment error	degree	0	0	0	0	0	0	0	0
Antenna Diameter	m	1.8	1.8	3.7	3.7	1.8	1.8	3.7	3.7
Illumination Efficiency	%	58	58	54.5	54.5	58	58	54.5	54.5
Andrew Ltd Model		P6F-17C	P6F-17C	P12F-17C	P12F-17C	P6F-17C	P6F-17C	P12F-17C	P12F-17C
Wavelength	m	0.1773	0.1773	0.1769	0.1769	0.1773	0.1773	0.1769	0.1769
Resulting Gain	[numeric]	590	590	2354	2354	590	590	2354	2354
Resulting Gain	dBi	27.71	27.71	33.72	33.72	27.71	27.71	33.72	33.72
Beamwidth	degree	7.55	7.55	3.78	3.78	7.55	7.55	3.78	3.78
Pointing Loss	dB	0.00	0.00	0.00	0.00	0.00	0.00	0.00	0.00
Minimum Gain	dBi	27.71	27.71	33.72	33.72	27.71	27.71	33.72	33.72
Sky Noise Temp	K	60	70	40	50	60	70	40	50
Feed Loss	dB	0.2	0.2	0.2	0.2	0.2	0.2	0.2	0.2
Pre-LNA Loss	dB	0	0	0	0	0.3	0.3	0.3	0.3
Total Loss	[numeric]	1.047	1.047	1.047	1.047	1.122	1.122	1.122	1.122
Physical Temp	Celsius	25	50	25	50	25	50	25	50
Resulting Noise Factor	[numeric]	1.048	1.053	1.048	1.053	1.125	1.136	1.125	1.136
Resulting Noise Figure	dB	0.205	0.222	0.205	0.222	0.513	0.554	0.513	0.554
LNA/Receiver Noise Figure	dB	0.4	0.4	0.4	0.4	0.4	0.4	0.4	0.4
System Noise Temp	K	103.35	114.53	83.35	94.53	127.77	140.82	107.77	120.82
Ageing & Other losses	dB	0.2	0.7	0.2	0.7	0.2	0.7	0.2	0.7
Resulting G/T minimum	dB/K	7.37	6.42	14.31	13.26	6.44	5.52	13.19	12.20
Margin (>0 for OK)	dB	1.37	1.42	0.31	1.26	0.44	0.52	-0.81	0.20

Table 2: G/T Calculation

In the interpretation of the requirements under US.190, it is understood that:

- The “nominal” case, with the higher G/T, represents the target when all of the receiver equipment is operating ideally.
- The “worst” case, with the lower G/T, represents the situation under adverse conditions (worst case equipment performance, old antenna, low elevation, etc).

Looking over the spreadsheet, the margins are positive for all configurations except for the one case, the HRUS with the optional pre-LNA filter under the “nominal” conditions, however, the margin under worst case is positive by 0.65dB.

Although there are some figures which are based on our judgement and previous experience, such as the sky noise temperature and the ageing allowance, the majority of the information is the worst case values from the various equipment suppliers.

The “feed loss” includes the LDF4-50A cable connecting the Andrew feed to the downconverter, this is quoted 0.103dB/m at 1.7GHz and we can use slightly less than 1m. The feed assembly insertion loss is probably less due to larger diameter, so a figure of 0.05dB is used, together with some allowance for connector mismatch at rounded figure of 0.2dB was used. We understand the quoted antenna gain already includes the feed loss, so only its influence on noise temperature is important. For simplicity, we include it as a separate term from the antenna gain.

The connectors used from the feed to the cable (“F” flange) and from the cable to the downconverter (N-type), provided they are kept clean and dry, should introduce negligible ohmic loss. Most of the effects are reflection loss, this is less damaging to noise temperature but has the same loss effect on gain. To account for this, and any possible degradation in this area over time, an estimated “ageing” term is included.

 VCS ENGINEERING	Meteosat Second Generation	 EUMETSAT
VCS/DADF/UST/DSP/016 Issue: 5.0 Date: 1999-08-23	DADF User Station Design Justification RF Front-End	EUM/MSG/SPE/128 Issue: 5.0 Date: 1999-08-23

The worst case ambient temperature is taken as +50°C for use in Africa, however, the effect of changing this (from the +25°C nominal case) on the overall G/T performance is small, typically around 0.04dB without the pre-LNA filter and 0.1dB with.

The pointing error used in the calculations is actually zero. This is due to the link budget provided by the spacecraft ICD allowing for loss due to pointing error (and polarisation rotation) already. We have retained this computation in the spreadsheet since it allows investigation of the alignment of the antenna, etc.

The mechanical adjustment requirement of US.220 depends upon the location of the reception site and any local horizon blockage (tall buildings, etc) which are not specified. However, the mechanical mount we would normally suggest can be adjusted from 0 degrees elevation to 85 degrees (higher is possible if the support legs are fixed to a tilted platform, for example a few M16 washers under one leg) and to any azimuth value, which should satisfy US.220. It should be noted that the G/T values are only specified for 10 degrees elevation and above.

The choice of the Andrew antenna models is based on their high quality, proven through out the world under adverse conditions, and our extensive experience of these designs in our numerous installations. The Andrew feed is not the highest illumination efficiency possible, however, it has very good sidelobe and backlobe performance and the “cupped dipole” design has reasonable attenuation of low frequency (below the equivalent waveguide cut-off frequency) transmissions (when compared to other designs, such as open dipole or patch antennas).

4.2 HRUS Antenna Results

It is our design solution to specify the 3.7m antenna (Andrew P12F-17C) for the HRUS. When combined with the very low noise downconverter, the resulting margin for operation is 0.31dB against the “nominal” case and 1.26dB against the “worst” case.

These may look health, however, (as outlined in our original proposal) we strongly advise the fitting of a pre-LNA filter to protect against interference in the increasingly crowded L-band. This is particularly true of the uplink site. If we consider the case with the 0.3dB insertion loss filter offered, the margin is -0.81dB in the nominal case, however, for the worst case conditions, the margin is positive by 0.20dB, an acceptable margin considering the worst case summation used.

4.3 LRUS Antenna Results

It is our design solution to specify the 1.8m antenna (Andrew P6F-17C) for the LRUS. This leads to a healthy margin of around 1.40dB without a pre-LNA filter and an acceptable worst case margin of 0.52dB if the optional filter is used.

4.4 Local Oscillator Performance

4.4.1 Choice of 1st LO Frequency

The choice of 1st LO frequency is determined by the need for:

- A) Low IF to simplify the signal processing.
- B) High IF to avoid image channel problems.

To satisfy US.270 we would propose to retain our conventional PDUS / MDD 1st LO of 1553.5MHz which results in HRIT on 141.65MHz and LRIT on 137.5MHz. This provides quite good image rejection with a reasonable RF filter (typically 50dB) and allows for some reverse compatibility with existing front-ends.

If the optional pre-LNA filter is used, the image channel rejection is greater than 100dB.

4.4.2 Frequency Stability

The long term stability of the 1st LO is important from the MUBM signal acquisition aspect, however, any improvement above that of the downlink will provide little improvement in overall system performance for the cost.

The most recent figures we have for the frequency stability are ±16ppm over the 7-year lifetime and an initial uncertainty of ±2ppm. These can be compared to the original values of ±20ppm and ±4ppm respectively.

 VCS/DADF/UST/DSP/016 Issue: 5.0 Date: 1999-08-23	Meteosat Second Generation DADF User Station Design Justification RF Front-End	 EUM/MSG/SPE/128 Issue: 5.0 Date: 1999-08-23
---	---	--

It has now become clear that these figures refer to the actual downlink, since the MSG uses two separate “master” oscillators, not a common one hence their frequency uncertainties and phase noise add directly, not acting as a translation effect. When compared to the alternative of a single master oscillator and two different frequency multiplication ratios, the degradation of the MSG system in terms of maximum frequency uncertainty is:

$$\Delta f = \frac{f_{LO1} + f_{LO2}}{|f_{LO1} - f_{LO2}|} \approx 8.5 \quad 19$$

Although the worst case extremes due to temperature are unlikely to occur at the same time. The relative degradation of the MSG system in terms of phase noise is:

$$\Delta\phi^2 = \frac{f_{LO1}^2 + f_{LO2}^2}{(f_{LO1} - f_{LO2})^2} \approx 37.4 = 15.7\text{dB} \quad 20$$

To minimise the cost of the 1st downconverter and the MUBM, standard XCOs are used. If we take the adjustment accuracy as 1ppm, the effect of temperature as 15ppm over the -20°C to +50°C operating range, and a value of 10ppm for 10 years ageing (no adjustment) the total frequency uncertainty can be calculated and is shown in Table 32:

Source	Effect (relative)	Effect (absolute)	Total
PGS Uplink (atomic reference)	< ±0.1ppm	0.2kHz	0.2kHz
MSG Spacecraft Initial Setting	±2ppm	3.4kHz	
MSG Spacecraft Time & Temp	±16ppm	27.1kHz	30.5kHz
1 st Downconverter Initial Setting	±1ppm	1.6kHz	
1 st Downconverter Temperature	±15ppm	23.3kHz	
1 st Downconverter Time	±10ppm	15.5kHz	40.4kHz
MUBM (similar to 1 st Downconverter)	±25ppm	3.5kHz	3.5kHz
Grand Total			74.6kHz

Table 3: 1st Frequency Stability Budget

From this we propose to modify the MUBM acquisition range (US.400) from ±50kHz to ±75kHz to avoid the high reproduction cost of an OCXO or TCXO solution.

4.4.3 Spectral Purity

The purity of the 1st local oscillator is important in two ways, firstly close in phase noise has an effect on the demodulator technology loss, our studies of the high coding gain QPSK system specified for HRUS indicate this is quite an important factor.

The second factor is phase noise and spuria at high offset frequencies since these effect the strong signal capability of the reception system ("reciprocal mixing").

There are a number of inputs to the phase noise specification, these are:

- The spacecraft ICD [AD9] specifies -49dBc/Hz @ 10Hz for the HRIT and LRIT transponder.
- The PSG specification calls for less than 2° from 10Hz to 1MHz (ANT.1300), although this ignores the EDA phase ripple.

	Meteosat Second Generation	
VCS/DADF/UST/DSP/016 Issue: 5.0 Date: 1999-08-23	DADF User Station Design Justification RF Front-End	EUM/MSG/SPE/128 Issue: 5.0 Date: 1999-08-23

- Our studies of the carrier recovery PLL showed that an overall model of -40.2dBc/Hz at 10Hz and -87.8dBc/Hz at 1kHz was acceptable.

From these figures, and the general requirement for cost effective engineering, we propose the following phase noise specification:

Offset Frequency Range	Phase Noise	Spuria
10Hz	< -45dBc/Hz	
1kHz	< -95dBc/Hz	
2MHz	< -135dBc/Hz	
< 330kHz		< -50dBc
330kHz to 50MHz		< -70dBc
> 50MHz (non-harmonic)		< -50dBc

Table 4: 1st Downconverter Oscillator Purity

The phase noise values at high offset frequencies are based on the other factors relating to strong signal handling, these could be improved, but would offer little advantage when the limitations of the other downconverter parts are considered (RF bandpass filter, LNA and Mixer overload limit, etc). For non-harmonic spuria beyond 50MHz the specification can be relaxed since the RF bandpass filter (100MHz bandwidth) cuts in and reduces the sensitivity to mixing products from any spuria in this range.

It should be stressed that most spectrum analysers, and some signal generators, are not capable of such performance, so it is not proposed to perform acceptance testing of the LO purity beyond an inspection on a standard spectrum analyser.

The computation and justification of the 1st LO XCO performance are included in the PLL design justification (for the 10Hz offset values) and the wideband figures are available from the cavity oscillator manufacturer's data.

The choice of a cavity oscillator phase locked to a VHF crystal reference oscillator was based on the minimum development cost to meet the high performance required here. It is unlikely that a single IC synthesiser with an LC or stripline oscillator would meet the -45dBc/Hz specification at 10Hz offset frequency, and the other option of a harmonic multiplier chain requires considerably more development effort.

4.5 Remote S-Meter Monitoring Facilities

The remote S-Meter of US.280 needs careful consideration since the working S/N ratio at the IF/baseband will be quite low, around 3dB, so there will be little peaking of the IF signal power and a serious penalty for incorrect adjustment. To make the display stable, a 0.6s average FIR filter will be used to minimise the 100rpm spin modulation. This is still a short time compared to the mechanical adjustment procedure for the antenna.

Before system phase lock is achieved the adjustment must rely on the IF power estimated from the incoherent AGC systems of the MUBM. This will only offer 3dB peaking so an expanded scale and the 0.6s integration period for stable readings will be essential.

To improve on this method, once phase and bit lock are achieved the "S-Meter" can display either an estimated S/N ratio from the demodulator coherent AGC system (for Es/No below the normal operating point) or the estimated channel error rate from the Viterbi decoder IC's internal BER monitor system for normal operation and higher Es/No. This will ensure adjustment based on the actual error rate. The HRUS, with the long (around 5s) lock up time is the more difficult system to adjust in this respect.

The Viterbi decoder BER monitor is based on comparing the (delayed) input symbols with the re-encoded output of the decoder (Qualcomm, 1992, p14-16), this provides a sensitive monitor of the Es/No from around -1dB (slightly below the CCSDS coding system operating point of -0.8dB) up to about 6dB.

	Meteosat Second Generation	
VCS/DADF/UST/DSP/016 Issue: 5.0 Date: 1999-08-23	DADF User Station Design Justification RF Front-End	EUM/MSG/SPE/128 Issue: 5.0 Date: 1999-08-23

Above this Es/No value and the number of channel symbol errors counted in the 0.6 second integration time is rather small, hence for adjustment above this value, the IF power alone (incoherent AGC) becomes a better adjustment measure. Considering the small margins for the MSG system, this final option for 7dB extra and above is not really necessary.

4.6 Test Signal Injection

The requirement for a test signal input (US.300) would have a significant G/T impact on the HRUS even if a high quality pre-LNA coupler with ~0.2dB insertion loss was used, so it is our design proposal to use a coupler after the LNA. This allows basic system testing but not full hardware testing since the LNA functionality would not be verified by the test signal.

The strict interpretation of US.300 requirement "without radiating" is impossible, but we assume that the isolation provided by this configuration, together with the proper screening of the components used in the downconverter, will be satisfactory.

We would not propose this feature for ordinary user stations. If such a test was required the antenna could be manually disconnected (normal N-type connector) and the test signal injected directly, possibly with a 30dB attenuator to allow a high signal level on the test signal cable to minimising the danger of picking up interference.

	Meteosat Second Generation	
VCS/DADF/UST/DSP/016 Issue: 5.0 Date: 1999-08-23	DADF User Station Design Justification MSG User Station Baseband Module	EUM/MSG/SPE/128 Issue: 5.0 Date: 1999-08-23

5 MSG User Station Baseband Module

5.1 Overall Architectural Approach

Beside the bottom up approach used for the evaluation of the signal conditioner described in the following subsection, the general approach of VCS is to design the MUBM as a modular system. Reasons for this are:

- To reduce the design risk as a modular system allows for flexibility in the case of re-combination of functions caused by physical or mechanical limitations for the board layout.
- To adjust computing performance modules can be added or removed to or from the system.

Furthermore HRIT and LRIT MUBM are based on the same hardware/firmware components although the performance requirements for LRIT are less critical. Reason for this is

- to reduce the design effort.

On the other hand it will be possible afterwards to streamline the LRIT MUBM design but not necessarily under the scope of the DADF contract.

In addition VCS intends to re-use the VCS I960-System well known to Eumetsat from the HRI Encryption Infrastructure and MTP Encryption Infrastructure projects. Reasons are:

- The availability of a modular bus-system including specification.
- The availability of the main processor board.
- The availability of firmware components, such as interface drivers, real-time kernel etc.
- The reduction of design risk for the above-mentioned items.

5.2 Design of MUBM Signal Conditioner

5.2.1 Overview

The proposed design of the MUBM signal conditioner covers the final IF, A/D conversion, demodulation and bit synchronisation. This has been studied in detail to achieve the low technology loss required of the MUBM for both the HRUS and LRUS, the details of these studies are included as two technical notes, one for the demodulation and the other for the bit synchronisation and matched filter design.

Throughout the theoretical study great care was taken to make reasonable estimates of those factors effecting the system technology loss and to compute and justify the system parameters in some detail.

In addition to the theoretical considerations there was a definite objective for the hardware design, to achieve high performance at reasonable cost. We believe the proposed design will exceed all of the EUMETSAT technical requirements while using standard, cost effective hardware.

The design of the carrier phase tracking system and the bit synchronisation system were based on the Harris HSP50214 "Programmable Downconverter". The proposed design uses the main sections of the HSP50214 to implement the most numerically intensive parts of the required signal processing algorithms:

- The A/D input level detector and internal AGC loops for signal level control.
- The demodulation section (mixer, NCO and CIC decimation filter) for the carrier phase tracking.
- The programmable FIR filter to implement the bulk of the baseband matched filters
- The polyphase filter & NCO to perform the timing adjustment required for bit synchronisation.

	Meteosat Second Generation	
VCS/DADF/UST/DSP/016 Issue: 5.0 Date: 1999-08-23	DADF User Station Design Justification MSG User Station Baseband Module	EUM/MSG/SPE/128 Issue: 5.0 Date: 1999-08-23

This VLSI chip is not really intended (by the manufacturers) for the high data rates of the HRIT transmission, however, for the HRIT parameters it proves to be an excellent solution when combined with suitable DSP software.

Our studies have shown the HRIT parameters to be quite critical for low technology loss, and the problem of the EDA phase ripple has been considered in as much detail as we had available. In addition, the use of the VLSI hardware and DSP software raised the issue of loop time delays; this is an important factor in the software architecture for the signal conditioner.

5.2.2 Design Parameters

The target for the design was for an overall technology loss of less than 0.8dB at the nominal MSG operating point ($E_b/N_o = 2.8\text{dB}$ from US.420). Provisionally this was divided into 4 main sources of potential technology loss:

1. Carrier phase tracking errors (thermal noise, link phase noise, and EDA phase disturbances).
2. Bit synchronisation-timing errors (thermal noise and timing quantisation).
3. Matched filter errors (ISI and frequency response errors).
4. Other sources (A/D errors, noise aliasing, quantisation errors, etc.)

The 3rd problem due to the signal filtering is separated in to two effects: The ISI term, the degradation in effective E_b/N_o due to ISI on the decision values used only, and the frequency response, the extra noise due to imperfect matching of the receiver filters. The 4th set of problems were not investigated in great detail since all of the hardware proposed have very high performance in all of these areas and should have a negligible effect on the overall performance. Our previous experience of receiver design (both analogue and digital) allows high confidence in this assumption.

During the design study and the analysis of the proposed hardware architecture the initial assumption was for no more than 0.2dB from each source, this has been achieved and the overall results from the theoretical study are included in the tables below (from the technical notes):

Parameter	HRIT	LRIT
RF Downlink	1695.15MHz	1691.00MHz
1 st LO Frequency	1553.5MHz	1553.5MHz
1 st IF Frequency	141.65MHz	137.5MHz
1 st IF Filter Bandwidth	4MHz	4MHz
1 st IF Filter Type	4 th Order Bessel	4 th Order Bessel
Image Rejection	> 55dB	> 55dB
2 nd LO Frequency	132.9MHz	128.75MHz
2 nd IF (A/D Input)	8.75MHz	8.75MHz
A/D Sample Clock Rate	35MHz	35MHz
Number of FIR taps	16	52
Total Filter ISI	-61dB	-64dB
ISI Loss	1.2E-5dB	5.4E-6dB
Frequency Response Loss	0.004dB	2.9E-4dB
Total Loss Assumed	< 0.05dB	< 0.05dB

Table 5: IF Frequency and Filter Design

 VCS/DADF/UST/DSP/016 Issue: 5.0 Date: 1999-08-23	Meteosat Second Generation	 EUM/MSG/SPE/128 Issue: 5.0 Date: 1999-08-23
	DADF User Station Design Justification MSG User Station Baseband Module	

Parameter	HRIT	LRIT	Comments
A/D (Input) Sample Rate	35MHz	35MHz	CLKIN = 52MHz maximum. Need not be synchronous with the processing clock. Our choice based on external EMC and complexity considerations.
Processor Clock	35MHz	35MHz	PROCCLK = 35MHz maximum.
Signal Bandwidth	976kHz	293.9kHz	$F_{MAX} = (1+a)/(2*T_S) =$ Low pass equivalent. RF/IF equivalent is twice this.
CIC Decimation Factor	5	14	$R_{CIC} = CLKIN / F_{CIC}$ Must be integer, range 4-32.
CIC Output Rate	7MHz	2.5MHz	$F_{CIC} = CLKIN / R_{CIC}$ Ideally be $8 * F_{MAX}$ for -84dB alias rejection.
Halfband decimation filters	Bypass	Bypass	[not used]
FIR Decimation Factor	2	2	$R_{FIR} = F_{CIC} / F_{FIR}$ Must be integer.
FIR Output Rate = F_{FIR}	3.5MHz	1.25MHz	Ideally $4 * F_{MAX}$, maximum limited to $PROCCLK / 6 = 5.833MHz$
Number of FIR taps	16	52	$N_{TAP} = \text{floor}(PROCCLK * R_{FIR} / F_{CIC} - R_{FIR}) * 2$ for symmetric, even, real filters.
FIR Time response	2.286µs 2.6 symbols	20.8µs 6.1 symbols	N_{TAP} / F_{CIC}
Polyphase Decimation Factor	1.52	2.13	F_{FIR} / F_{SAMP} , non-integer adjusted for bit sync, range 1-4
Polyphase Output Rate	2.296MHz	587.8kHz	$F_{SAMP} = 2 \text{ Sample / Symbol exactly.}$
Halfband Interpolation Filters	Bypass	Bypass	[not used]
Frequency Discriminator	-	-	[not used]

Table 6: HSP50214 Configuration Parameters

The symbol rates are based on an overhead of 4 bytes sync word and 4*32 bytes R/S check symbols per 1024 byte CCSDS frame. This results in 256/223 for the total frame overhead. The R=1/2 convolution coding doubles this symbol rate, however, in the QPSK case two symbols are sent per "bit clock" cycle. This results in 1Mbit/sec packetised data rate for HRIT translating in to a nominal symbol clock rate of 1.147982MHz and the 128kBit/sec of LRIT resulting in a nominal symbol clock rate of 293.883kHz.

 VCS/DADF/UST/DSP/016 Issue: 5.0 Date: 1999-08-23	Meteosat Second Generation DADF User Station Design Justification MSG User Station Baseband Module	 EUM/MSG/SPE/128 Issue: 5.0 Date: 1999-08-23

Parameter	Acquisition	Tracking
Type	Costas loop ($M^2 \sin(4\theta)$ non linearity) on all I/Q samples. 2 nd Order, type 2 loop filter.	Costas loop ($M^2 \sin(4\theta)$ non-linearity) on optimum (data decision) I/Q samples. 2 nd Order, type 2 loop filter.
Natural Frequency	180Hz	128Hz
Damping Factor	1.14	1.14
Sweep Rate	20kHz/sec	N/A
Lock Detect Filter	50ms	100ms
Technology Loss	N/A	0.08dB

Table 7: HRIT QPSK Loop Parameters

It is worth noting that an acceptable range of operation (say, less than 0.2dB loss) for HRIT occurs for natural frequencies between 80Hz and 200Hz. This minimum is quite sharp since the system is operating close to the acceptable limit. The consequence of this sensitivity to the performance of the system is the requirement for a good AGC system to maintain operation at the correct signal levels so the PLL parameters are accurately maintained near the optimum value.

Parameter	Acquisition	Tracking
Type	Costas loop (2 nd power) on all I/Q samples. 2 nd Order, type 2 loop filter.	Costas loop (2 nd power) on optimum I/Q samples. 2 nd Order, type 2 loop filter.
Natural Frequency	400Hz	140Hz
Damping Factor	1.14	1.14
Sweep Rate	200kHz/sec	N/A
Lock Detect Filter	50ms	100ms
Technology Loss	N/A	0.04dB

Table 8: LRIT BPSK Loop Parameters

Parameter	HRIT	LRIT
Timing Error Algorithm	ZCD (on I data only)	ZCD
PLL Natural Frequency	233Hz	83Hz
PLL Damping Factor	1.14	1.14
Bit Rate Frequency Range	± 250 Hz	± 100 Hz
Technology Loss	< 0.025dB	< 0.025dB
Operation with EDA failure	Yes	Yes

Table 9: Bit Synchroniser Characteristics

 VES ENGINEERING	Meteosat Second Generation DADF User Station Design Justification MSG User Station Baseband Module	 EUMETSAT
VCS/DADF/UST/DSP/016 Issue: 5.0 Date: 1999-08-23		EUM/MSG/SPE/128 Issue: 5.0 Date: 1999-08-23

5.2.3 Summary of Technology Loss Terms

The following table summarises the losses accounted for during the study of the theoretical design and the hardware limitations of the proposed architecture:

Parameter	HRIT	LRIT
Carrier Tracking Errors (including EDA phase ripple)	0.08dB	0.04dB
Matched Filter Errors (including final IF filter)	0.05dB	0.05dB
Bit Timing Errors	0.025dB	0.025dB
Total	0.16dB	0.12dB

Table 10: Technology Loss

From the computed performance of the system, we are confident that both HRUS and LRUS designs will meet the 0.8dB technology loss design specification. The system should also track carrier and clock through a 3dB dip from a faulty EDA element; of course, the recovered user data would be unusable during this period.

5.2.4 Hardware Architecture

The design is based on a combination of analogue and digital hardware and is illustrated in figure 1 below. This diagram excludes the M&C path for the remote S-Meter.

The 2nd frequency conversion stage and analogue AGC system are design to make optimum use of the 10 bit flash A/D converter used to sample the final IF signal.

From this point on the sampled data is processed and reduced to two samples per symbol by the HSP50214 VLSI chip, this implements the demodulation phase tracking, matched filter and symbol timing interpolation.

Finally the DSP software implements the carrier phase detector and loop filter, and the bit timing error detector and loop filter. The resulting symbol soft decisions are then forwarded the Qualcomm VLSI Viterbi decoder, which implements the inner decoder of the FEC system.

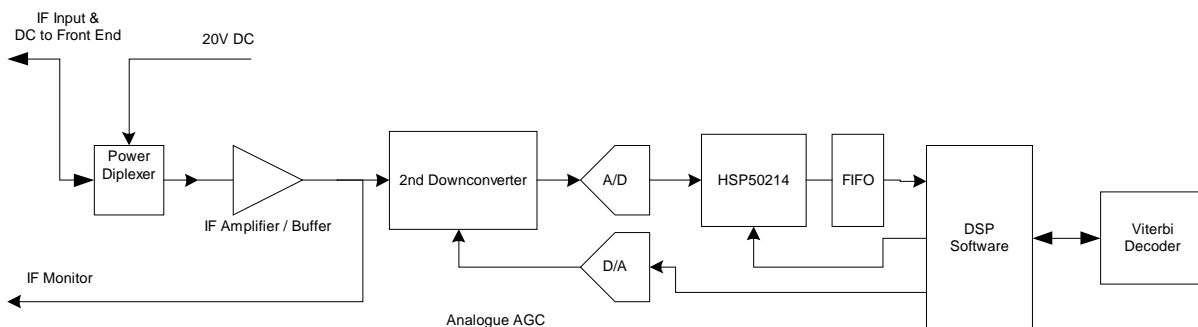


Figure 3: MUBM Signal Processing Block Diagram

5.2.5 FIFO Buffer Requirements

The FIFO buffer provides for the difference in the continuous rate data from the HSP50214 (the 16-bit I & Q samples) and the block processing software requirements. During the study of the PLL it was found that time delay within the PLL was very important and the maximum tolerable delay was 100µs.

For a block transfer, the mean delay is approximately half of the period of the buffer, however there is some time required to update the PLL filter states and to transfer back to the HSP50214. In the worst case (assuming the DSP processor is working near maximum for these tasks alone), the time from "end of buffer" to computation completed could be 90% or so of the buffer block time. Hence the average delay could vary between 1 and 1.5 blocks depending on the CPU utilisation.

 VES ENGINEERING	Meteosat Second Generation DADF User Station Design Justification MSG User Station Baseband Module	 EUMETSAT
VCS/DADF/UST/DSP/016 Issue: 5.0 Date: 1999-08-23		EUM/MSG/SPE/128 Issue: 5.0 Date: 1999-08-23

For these reasons, we propose to make the buffer depth 67% of the maximum delay, although with the fast DSP system planned this could be increased to 90% or so.

In the case of the HRIT data, the period of 67µs represents 78 symbol pairs (I&Q in parallel) (156 samples).

In the case of LRIT data, this is 20 symbols (40 samples).

These are much shorter than the ideal for efficient interrupt service and DMA operation, however, this constraint is part of the most cost-effective solution.

The implementation of this buffer needs consideration, if this implemented entirely in software (via the DSP's DMA controller), the reprogramming of the DMA system must be completed in under one sample period, which is 0.43µs for HRIT, a demanding specification on interrupt latency, etc. To ease this, a small (perhaps 16 word) 256 word hardware FIFO ~~is could be~~ used to increase the window to 7110µs, which is then easy to satisfy.

To simplify the processing code, the buffer ~~will probably be implemented as a "ping-pong buffer" with two arrays in memory (swapped on each transfer completion), rather than as is implemented as a "circular ring buffer" but with block updating of the read/write pointers.~~

The expected CPU utilisation is illustrated in the following figure.

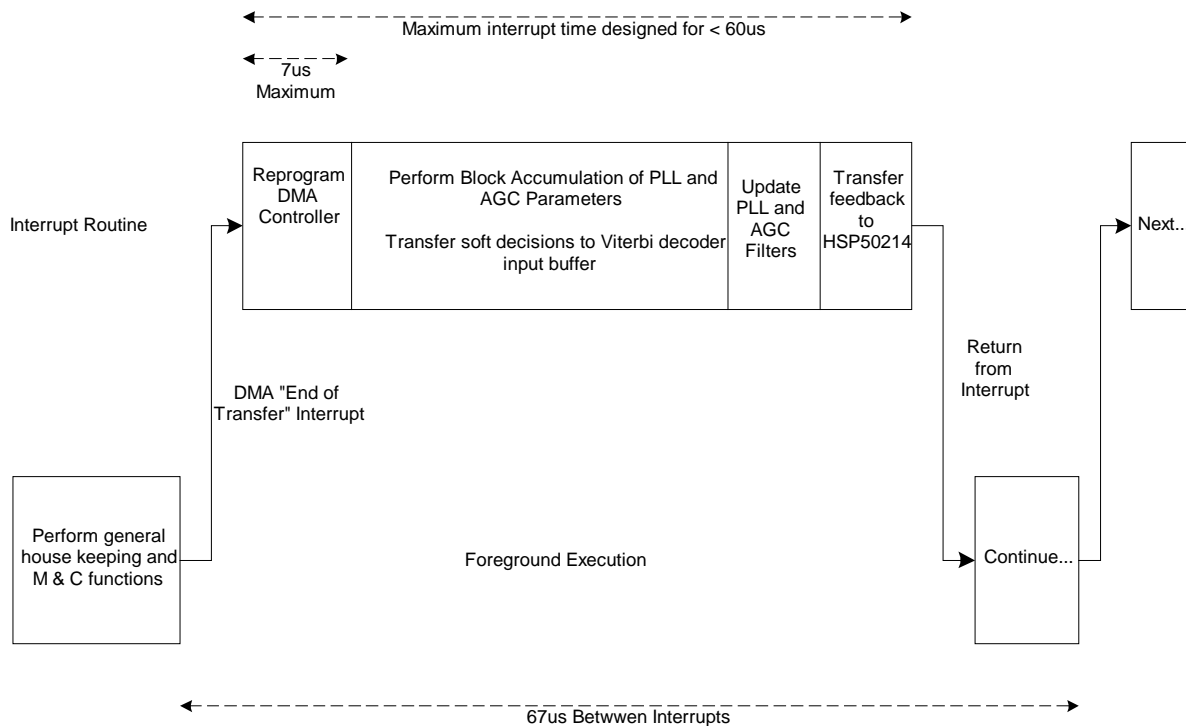


Figure 4: DSP Software CPU Load Diagram

5.2.6 Carrier Phase Error Algorithm

5.2.6.1 HRIT System

The study of the HRIT QPSK receiver and the EDA phase ripple showed significant care was needed to achieve high performance. In this case the phase estimation non-linearity is given by:

$$v_E = I \cdot Q \frac{I^2 - Q^2}{I^2 + Q^2}$$

 VES ENGINEERING	Meteosat Second Generation	 EUMETSAT
VCS/DADF/UST/DSP/016 Issue: 5.0 Date: 1999-08-23	DADF User Station Design Justification MSG User Station Baseband Module	EUM/MSG/SPE/128 Issue: 5.0 Date: 1999-08-23

This is not a trivial task to compute in real time. In addition, the QPSK carrier lock detection system requires consideration, this, when combined with the need for coherent AGC for accurate PLL operation, leads to the $\text{Re}\{z^4\}$ form of:

$$v_{LD} = Q^4 - 6 \cdot I^2 \cdot Q^2 + I^4 \quad 22$$

If we use integer maths there is a danger of the x^4 effect causing overflow, possible with 8 bit I & Q data and a 32 bit register for computation. The use of floating point math avoids this, but there is still a danger of $I=Q=0.0$ causing a divide by zero exception (unless tested before computed). In either integer or floating point maths there is a divide, normally a time consuming operation. In total this would require 4 multiply, 2 add/subtract, 1 zero test and 1 divide operation per I/Q sample pair.

We could do the computation for both terms in real time, this is illustrated in the following 'C' code fragment.

```

if(vi == 0 && vq == 0){
    ve = vld = 0;
} else {
    vi2 = vi*vi;
    vq2 = vq*vq;
    ve = vi*vq*(vi2 - vq2)/(vi2 + vq2);
    vld = vq2*vq2 - 6*vi2*vq2 + vi2*vi2;
}

```

Figure 5: Direct Computation of QPSK Non-Linearity

If performed in integer maths, greater care is needed to scale the input terms and check the order of evaluation to minimise the chance of overflow or loss of precision.

Estimating the CPU load from the high level code is not easy, since it depends on the instructions used by the compiler, register allocation, etc, however we can make a typical guess for a standard RISC processor. In the above example, there are about 14 "standard" instructions plus a divide, which can take 32-64 CPU cycles to execute. Clearly this represents a high CPU load, particularly for the initial search when bit synchronisation is not achieved and all input samples must be processed, here we have possibly 90-180MIPS demand for this task.

Clearly the CPU must be capable of more than this, so the computation is completed in less than the real-time equivalent rate. There are other tasks to be performed, both in the interrupt handler and in the foreground execution.

To reduce this problem, the standard approach is the use of a pre-computed look up table (LUT). This trades off memory for CPU effort, unfortunately we have two signals (I & Q) and a 2 dimensional LUT requires much more memory to implement. There is an additional consideration, if the DSP processor is required to go to off-chip memory this greatly reduces the execution speed, this, rather than the total memory available to the system, is the greatest consideration.

Considering this, we have to scale and limit the I & Q signals to make optimum use of memory. Depending on the compiler, it may be sensible to implement the address indexing in the high level code to have efficient operation.

 VCS ENGINEERING	Meteosat Second Generation DADF User Station Design Justification MSG User Station Baseband Module	 EUMETSAT
VCS/DADF/UST/DSP/016 Issue: 5.0 Date: 1999-08-23		EUM/MSG/SPE/128 Issue: 5.0 Date: 1999-08-23

The LUT approach results in code similar to:

```

phase_error = agc_level = 0;
if(bit_lock) {
    ii_start=1; /* Data decisions on odd index so */
    ii_inc=2; /* if Bit sync achieved, use optimum samples only. */
} else {
    ii_start=0;
    ii_inc=1; /* No bit sync, use all samples. */
}
for(ii = ii_start; ii<BLOCK_SIZE; ii += ii_inc) {
    vi = (unsigned)data[ii].i >> LUT_SHIFT;
    vq = (unsigned)data[ii].q >> LUT_SHIFT;
    non_lin_info = error_lut[vi][vq]; /* Recover Ve and Vld */
    phase_error += non_lin_info.ve;
    agc_level += non_lin_info.vld;
}

```

Figure 6: Carrier and AGC Code Example

Here it is assumed that `data[0..BLOCK_SIZE-1]` is the zero offset array used for the current (full) I & Q buffer, with structure members `.i` and `.q` respectively. The parameter `BLOCK_SIZE` is the number of samples in the FIFO, arranged with even index = middle of bit cell and odd index = edge of bit cell (the bit sync will adjust the timing re-sampling until this is true).

In the above example, the code requires about 10-12 instructions per loop. Before bit sync is achieved this requires around 27MIPS, after bit sync is achieved this reduces to about 13MIPS. Note that the accumulated values will be double in the unlocked case, so the filter constants need to be changed accordingly.

5.2.6.2 LRIT System

The study of the LRIT BPSK receiver and the EDA phase ripple showed no problems in the implementation. In this case, the 2nd power phase estimation non-linearity is given by:

$$v_E = 2 \cdot I \cdot Q \quad 23$$

although the factor of 2 is not required, it is absorbed by the loop filter constants. The coherent ACG and lock detect term is given by:

$$v_{LD} = I^2 - Q^2 \quad 24$$

These are simple and could be computed in real time with no problems, however, there is an attraction in using the same LUT based code as the HRIT design to implement the required equations. Direct computation would require about 7 instructions per sample processed. Without bit lock this is approximately 4MIPS (all samples) and 2MIPS with bit sync.

5.2.7 Bit Timing Error Algorithm

The Zero Crossing Detector (ZCD) was chosen since it is a simple algorithm, requires only matched filter samples (no derivative filter), and is easily implemented in the DSP software. Our studies have also shown it to perform within 2.6dB of the theoretical limit for the HRUS (2.2dB for the LRUS). It is our intention to use

	Meteosat Second Generation	
VCS/DADF/UST/DSP/016 Issue: 5.0 Date: 1999-08-23	DADF User Station Design Justification MSG User Station Baseband Module	EUM/MSG/SPE/128 Issue: 5.0 Date: 1999-08-23

the I channel only for HRIT, this is acceptable (from considering Gaussian timing errors) and leads to common code (but with different parameters) for both the HRUS and LRUS bit synchroniser.

The basic ZCD algorithm involves detecting a data transition from the optimum samples (at the current symbol, $t = n$ and the previous symbol at $t = n-1$) and using this to direct the error voltage observed at the mid point ($t = n-\frac{1}{2}$):

$$v_E = x\left(n - \frac{1}{2}\right) \left[\text{sign}(x(n)) - \text{sign}(x(n-1)) \right] \quad 25$$

where $x(t)$ is the observed signal and noise from the matched filter and interpolator.

For the bit timing alone, the following figure shows a 'C' code example to illustrate the possible implementation. In practice, however, the software would probably run through each block in the FIFO buffer accumulating the total errors (for carrier and clock) together with AGC and lock detect information.

```

timing_error = 0;
for(ii = 1; ii < BLOCK_SIZE; ii += 2) {
    if(last_symbol < 0) {
        if(data[ii].i > 0) timing_error += data[ii-1].i; /* 0-1 transition */
    } else {
        if(data[ii].i < 0) timing_error -= data[ii-1].i; /* 1-0 transition */
    }
    last_symbol = data[ii].i; /* Save for next block processing operation. */
}

```

Figure 7: Bit Sync ZCD Timing Error Detector Code Example

Here it is assumed `last_symbol` is static between block processing calls. In the above case, we have about 10 cycles per symbol, although a good compiler might reduce this to 6 or so. If the carrier phase error code was included, the `for()` loop indexes both with no extra effort, however, this might reduce the optimisation performed by the compiler if the code becomes too complex.

Based on this estimate, we have about 11MIPS for HRIT bit sync and 3MIPS for the LRIT.

After this loop, the accumulated `timing_error` value (in 32 bit integer, to avoid overflow from the 16 bit I & Q data) would be applied to the bit sync loop filter, which implements the standard 2nd order filter. The Laplace transform of the standard 2nd order filter is:

$$F(s) = \left(\frac{A'}{s} + B' \right) \quad 26$$

Where A' (representing integration) and B' (representing direct gain) are chosen to suit the PLL dynamics required. In a sampled data system, integration becomes a running summation. This is illustrated by the following 'C' code example:

	Meteosat Second Generation	
VCS/DADF/UST/DSP/016 Issue: 5.0 Date: 1999-08-23	DADF User Station Design Justification MSG User Station Baseband Module	EUM/MSG/SPE/128 Issue: 5.0 Date: 1999-08-23

```

bit_accumulator += BIT_A * timing_error;
if(bit_accumulator > MAX_BIT_ACC)
    bit_accumulator = MAX_BIT_ACC;
else if (bit_accumulator < MIN_BIT_ACC)
    bit_accumulator = MIN_BIT_ACC;
bit_NCO_out = bit_accumulator + BIT_B * timing_error;

```

Figure 8: Bit Sync Loop Filter Code Example

Where `BIT_A` and `BIT_B` are the bit sync PLL filter constants. The upper and lower limits set the lock range for the PLL. This can be exceeded this by the B term, but not by any significant amount. Depending on the detailed design (where integer and floating point math details are considered), there may be scaling of the `bit_NCO_out` to improve the resolution, etc, of the A and B terms.

This requires around 7 instructions per update, for the 15kHz FIFO update rate (common to HRUS and LRUS) this implies a negligible loading of 0.11MIPS. The loading will probably be doubled by the time required to format and send this feedback value to the HSP50214.

The AGC and lock detect filters have similar complexity and update rate, hence similar (negligible) CPU loading.

5.3 Design of the Decoder

There are two functions for the decoder part, which require high performance in the HRIT case:

- Frame Synchronisation
- Reed Solomon Decoding

A rough estimation of the performance figures for RS decoding leads to 50 to 100 MIPS for the HRIT case. The frame synchronisation is less critical based on our experience of a HRPT frame synchroniser, which is realised on the I960-PB system. Anyway the computational burden is either on the frame synchroniser in the non-locked state or the RS decoding, when the frame synchroniser has only to check the lock.

Due to these performance figures, the TMS320C6201 will have sufficient computing performance for these functions. The general design of a processor board based on this DSP similar to the signal conditioner DSP part is reasonable.

5.4 Design of the PN Generator

The DES PN generator was originally foreseen to be implemented on the I960-DSP board. Due to performance results based on an Intel platform implementation, the PN generator was shifted to the software part of the user station system.

	Meteosat Second Generation	
VCS/DADF/UST/DSP/016 Issue: 5.0 Date: 1999-08-23	DADF User Station Design Justification Software	EUM/MSG/SPE/128 Issue: 5.0 Date: 1999-08-23

6 Software

The functionality of the user station software is specified by the requirements defined in the [FRS]. The data flow models could be arranged in several different ways. The following shall describe the main aspects of our architectural software design approach.

Online Buffer

One major aspect is the “online” buffer keeping all different processing stages of LRIT or HRIT files. Due to the requirements there is a need for a manual access to all stages of processed data of up to an hour history. In order to avoid unnecessary processing, all data of all stages are stored in the online buffer.

The user shall be able to manually copy data from the online buffer to the offline for long-term storage, as the online buffer will be purged regularly according to different mechanisms.

Offline Buffer

The offline buffer is implemented due to the above-mentioned requirement for long-term storage and in addition to store data, i.e. XRIT files, which matches the multi-entry filter. This mean can be used for debugging and analysis of data for the DADF facility.

In the nominal case, this filter would not include any entry. In the case of erroneous XRIT files w.r.t. compression/decompression and/or encryption/decryption, but not w.r.t. erroneous reception, dedicated files can be stored into the offline buffer via the multi-entry filter mechanism.

Herewith the reason for non-purging is given. The user shall be able to evaluate and assess the data items later at any time, maybe to transfer the data by different means to the DADF OFO for further analysis.

The configuration of the multi-entry filter could result in an enormous data stream when configured like “*”=“transfer all files in all processing stages”. This is the main reason for not to transfer the filtered data via a network to the DADF.

Storage Size and Buffer Access

As shown in section 3.1.2, the storage size and the access data rates cannot be neglected for the HRIT case. Due to this special care is taken for the design of the administration process of the online storage in order to minimise the need for writes.

	Meteosat Second Generation	
VCS/DADF/UST/DSP/016 Issue: 5.0 Date: 1999-08-23	DADF User Station Design Justification Simulators and Test Equipment	EUM/MSG/SPE/128 Issue: 5.0 Date: 1999-08-23

7 Simulators and Test Equipment

7.1 User Station Test Harness

The proposed User Station Test Harness will fulfil the corresponding requirements.

The User Station is sub-divided into LRUS and HRUS and therefor both systems are independent. Hence they can be tested independently. Accordingly there is no need for a test harness providing HRIT and LRIT data streams in parallel.

The interface data rates can be set up to either HRIT or LRIT rate. No other frequency shall be allowed. This is due to the fact, that the bespoke hardware of the MUBM is designed only according to these data rates. Doubling of data rates is not foreseen.

For the DADF tests a further simulator is foreseen. The User Station simulator shall be used to test the DADF in absence of the US. Here the closed loop between the output of DISE and the input of corresponding US monitoring data is tested via the PGS and the US simulator in real-time.

This is different for the US test harness. It shall be not designed for accepting and processing the VCDUs from the PGS simulator in real-time.

7.2 MUBM Testmodulator

The MUBM testmodulator allows for testing the critical performance aspects of the MUBM. This section provides a theoretical justification for the measurement accuracy of the test equipment.

7.2.1 Principles

In principal, the measurement of technology loss is simple. However, the practical task of performing the test requires great care. Our proposed measurement method follows this method:

- 1) Apply the test signal and adjust the level until an appropriate error rate is found. The MUBM is specified at a 5E-5 probability of frame failure (1 in 20,000 from US.540) but this leads to an unacceptably long test time to maintain a constant Eb/No input level. It is our proposal to perform the test at a frame failure rate of 1E-1 to 1E-2, thus allowing a reasonable number of error events (say, 100) in an acceptable time.
- 2) Determine the input Eb/No. In our proposal, this is calculated from the spectrum analyser measurement of the Y-factor between the (Signal+Noise) and the Noise, knowing the power spectral density characteristics of the signal.
- 3) Compare the Eb/No from the theoretical curve and (1), with the measurement (2), to arrive at the technology loss for the system.

7.2.2 Error Rate Determination

There are several ways of "measuring" the error rate. Although the basic specification is normally the bit error rate, in a packet-orientated system it is really the frame failure rate that matters. This can be obtained from one of the following methods:

- Directly by checking for frames in error with respect to the original data. This is the most certain method as it tests the frame integrity without any assumptions.
- Indirectly by the R/S decoding "failed" results. This *assumes* the implementation of the R/S decoder is correct and the "undetected" patterns of errors are rare. This is a good method once the system has been verified by the first method. In addition, it can be applied to "unknown" data during normal operation.
- By inference from the R/S decoding results when there are too few failures for reliable statistics. This

 VCS/DADF/UST/DSP/016 Issue: 5.0 Date: 1999-08-23	Meteosat Second Generation DADF User Station Design Justification Simulators and Test Equipment	 EUM/MSG/SPE/128 Issue: 5.0 Date: 1999-08-23
---	--	--

makes greater assumptions about the statistics of the Viterbi output and extrapolates from the high number of correctable events to compute the probability of the small number of uncorrectable events. This makes significant assumptions about phase noise, PLL behaviour, etc., but is acceptable in helping to extrapolate data obtained by one of the above methods to low error rates.

Due to the test requirement on EDA failure mode, we would propose the first method on the trace buffer. Since the EDA failure will be simulated synchronous to a pattern of repeating frames, all three methods could be the first two methods are applied on a “frame number basis” to show effectively the error rate as a function of spacecraft spin position. This would verify the requirement of US.402 with great precision, as well as the correct R/S decoder implementation.

At moderately low error rates we can estimate the error rate by the observing the interval containing N error events. In general, the standard deviation σ for N independent observations of p occurring is:

$$\sigma = \sqrt{\frac{\sum_{i=1}^N (\bar{p} - p_i)^2}{N - 1}}$$

So the relative error in the mean value (\bar{p}) is decreased by the factor of $\sqrt{\frac{1}{N-1}}$ and obviously at least two observed errors are required before it is possible to determine the interval(s) between them. The use of $N-1$ rather than N in the denominator is due to the lack of *a priori* knowledge of the mean value, to quote from (Numerical Recipes in ‘C’, 1992, p611) on this subject:

"We might also comment that if the difference between N and $N-1$ matters to you, then you are probably up to no good anyway - e.g., trying to substantiate a questionable hypothesis with marginal data."

Realistically a 2σ (95% confidence) accuracy of about $\pm 20\%$ (or better) in estimating the mean value is desirable, this requires 100 or more observed errors so σ is less than 0.1

Applying this to the MUBM test we would require about $100 \times 20000 = 2E6$ frames for the nominal operating point of $5E-5$. For HRIT (140.134 frame/sec) this is about 4 hours, and for LRIT (17.937 frame/sec) this is 31 hours!

The use of smaller numbers of detected frame failures is possible and the VCDU trace buffer analysis program automatically computes the 90% confidence limits for the error rate estimate. Details of this calculation, together with some of the numerical issues involved, are given in the test tools documentation.

Hence our proposal to measure at error rates of about $1E-1$ to $1E-2$, this requires 10^3 to 10^4 frames, taking about 7-70 seconds for HRIT and 1-10 minutes for LRIT. In addition, this tests the R/S throughput and the PLL systems under more difficult conditions than normal, ensuring thorough testing of the MUBM.

7.2.3 Eb/No Measurement

This is more difficult than it first appears since the SNR must be measured to high accuracy on the signal and the noise, with different probability distribution functions. Anyone who has used a spectrum analyser to measure signals will be familiar with the high amplitude resolution and the ease in deciding exactly what the instrument is observing. However, most RF spectrum analyser’s use a logarithmic detector, this is not the same as the true RMS characteristic needed for correct comparison of signals with different PDFs (the difference is significant, about 2.5dB for Gaussian against pure carrier). In addition, the noise bandwidth of the IF strip (the “resolution bandwidth”, or RB) is needed if absolute power measurements on noise (or noise-like) signals is performed.

This can be avoided by our proposed Y-factor method. Here the ratio of the S+N to N is observed by the power ratio close to the “carrier” of the simulated RF signal. This uses a narrow RB (relative to the signal power

 VES ENGINEERING	Meteosat Second Generation DADF User Station Design Justification Simulators and Test Equipment	 EUMETSAT
VCS/DADF/UST/DSP/016 Issue: 5.0 Date: 1999-08-23		EUM/MSG/SPE/128 Issue: 5.0 Date: 1999-08-23

spectrum) so the actual value is not important for such ratio measurements.

In addition, the narrow filtering of the simulated signal makes the PDF in the IF strip virtually Gaussian, hence the IF detector characteristic is not important. (In fact, narrow band filtering of a digital PN sequence is the normal method of generating accurate Gaussian noise). Even though, the spectrum analyser should be set to the “sampling” IF detector and not the normal “peak detect” as this would emphasise small differences in PDF.

Considering the simplest test signal, random synchronous NRZ-L data of $\pm V$ volts, there is (for this case) a power spectrum found from the Fourier transform of the autocorrelation function, given by:

$$|S(f)|^2 = V^2 T \text{sinc}^2(\pi f T)$$

Where T is the bit period and $\text{sinc}(x) = \frac{\sin(x)}{x}$. For a normalised 1Ω system, we have:

$$|S(f)|^2 = E_B \text{sinc}^2(\pi f T)$$

Hence if the ratio of the signal power density to the noise power density at $f=0$ could be measured (or the centre frequency for the bandpass equivalent signal), the value of E_B/N_O can be found.

What we observe is the SNR “Y-factor” (power ratio) measured by the spectrum analyser:

$$Y_{SNR} = \frac{\text{signal} + \text{noise}}{\text{noise}} = \frac{\int \left[|S(f)|^2 + N'_O \right] |R(f)|^2 df}{\int N'_O |R(f)|^2 df}$$

Where $R(f)$ is the frequency response of the spectrum analyser’s RB filter and N'_O is the observed noise density (due to the 1st IF signal and the spectrum analyser internal noise).

The noise density alone required in the denominator can be measured by switching off the simulator, or in the spectral nulls at integer multiples of the symbol rate. If we now assume $R(f)$ is very narrow, so $S(f)$ and N_O are essentially constant over the pass-band of $R(f)$, we have:

$$Y_{SNR} = \frac{\left[|S(f)|^2 + N'_O \right] \int |R(f)|^2 df}{N'_O \int |R(f)|^2 df}$$

Then assuming we are measuring at the peak signal where the “carrier” is, $f=0$ so we have:

$$Y_{SNR} - 1 = \frac{|S(0)|^2}{N'_O} = \frac{E_B \text{sinc}^2(0)}{N'_O}$$

Since $\text{sinc}^2(0) = 1$ this simplifies to E_B/N'_O . In extending this to the MUBM test, we must note this is the really the coded E_s/N_O value, so a code rate correction of 512/223 or 3.61dB is required. The function relating power density [at zero offset frequency](#) to E_s is 1 for BPSK and root-raised cosine filtering (as for unfiltered NRZ), but 2 for QPSK (since the equivalent power is effectively modulated in to half of the BPSK bandwidth).

We see how the RB cancels in final result, a useful simplification. What remains is the power ratio together with

 VES ENGINEERING	Meteosat Second Generation DADF User Station Design Justification Simulators and Test Equipment	 EUMETSAT
VCS/DADF/UST/DSP/016 Issue: 5.0 Date: 1999-08-23		EUM/MSG/SPE/128 Issue: 5.0 Date: 1999-08-23

the determination of $S(0)$, either from theory (proposed here) or by additional measurement.

To find the true noise density, we measure the Y-factor of the noise on the spectrum analyser when connecting to the MUBM IF test port. In this case we have:

$$Y_{SA} = \frac{S_{Anoise} + IF_{noise}}{S_{Anoise}} = \frac{N_{SA} + N_O}{N_{SA}} = \frac{N'_O}{N_{SA}}$$

This can be rearranged to obtain:

$$N'_O = N_O \frac{Y_{SA}}{Y_{SA} - 1}$$

Combining with the expression for the E_B/N_O term we end up with:

$$\frac{E_B}{N_O} = \frac{Y_{SNR} - 1}{\text{sinc}^2(0)} \left(\frac{Y_{SA}}{Y_{SA} - 1} \right)$$

As mentioned before, for non-BPSK/NRZ systems the $\text{sinc}^2(0)$ term must be replaced with the appropriate power spectrum value. Usually the spectrum analyser noise is small, so the Y_{SA} term is large (10-1000 for Y-factors of 10dB to 30dB) and the correction due to this effect small (0.45dB to 0.004dB).

All of these simple calculations are implemented in an EXCEL spreadsheet to ease the test procedure. After setting up the spectrum analyser and making the Y-factor measurements, the spread sheet computes the E_B/N_O that can be compared with the error rate estimate from the VCDU trace buffer analysis.

7.2.4 Analysis of Accuracy

The identified sources of error are:

- 1) Measurement of Y_{SNR} (spectrum analyser linearity).
- 2) Correction of spectrum analyser measurements (Y_{SA}).
- 3) Amplitude stability during the test.
- 4) Accuracy of simulated signal.
- 5) Measurement uncertainty of BER and effect on theoretical E_B/N_O

The 1st term is the dominant one. The catalogue specification for a typical spectrum analyser is not very helpful, what is required is the linearity for small Y-factors. Since we will be testing at E_B/N_O of around 2.8dB, this translates in to an E_S/N_O of around -0.8dB or a numerical Y-factor of 1.832 (about 2.6dB) in the LRIT case, or 2.66 (4.25dB) in the HRIT case.

If we have an accuracy of 0.1dB from the spectrum analyser (realistic, even if we need to use the DSP signal generator to perform a linearity verification), this is a ratio error of 1.0233. This leads to an error in the determination of E_B/N_O of about 0.2dB in the LRIT case and 0.16dB in the HRIT case.

For the 2nd term, the noise of the spectrum analyser must be considerably less then the measured signal, if this is 20dB (typical case) then the effect on the observed noise floor is less than 0.043dB. This can be measured with reasonable accuracy, say ± 1 dB, and the measurement correction is determined to about ± 0.01 dB.

In addition to the spectrum analyser accuracy, there is the question of the stability of the E_B/N_O during the

 VES ENGINEERING	Meteosat Second Generation DADF User Station Design Justification Simulators and Test Equipment	 EUMETSAT
VCS/DADF/UST/DSP/016 Issue: 5.0 Date: 1999-08-23		EUM/MSG/SPE/128 Issue: 5.0 Date: 1999-08-23

duration of the test (the 3rd term in the budget). Clearly we require as short a test as practical (outlined above) and some method of verifying stability. By maintaining constant temperature during the test (1 hour warm up, doors closed throughout, etc) and by measuring the Y-factor before and after the test, this should be better than 0.05dB.

The 4th term is essentially ignored, but set to 0.01dB to allow for quantisation noise, etc., in the generation of the simulated signal.

The 5th term depends on the number of observed errors (i.e. the test length). If we proceed with the assumption of 100 frame errors, leading to a 95% confidence of $\pm 20\%$ on the frame failure rate, we need to convert this in to an equivalent delta of E_B/N_O . This can be derived from the theoretical curve (actually determined by Viterbi simulation and theory) shown in Figure 5 below:

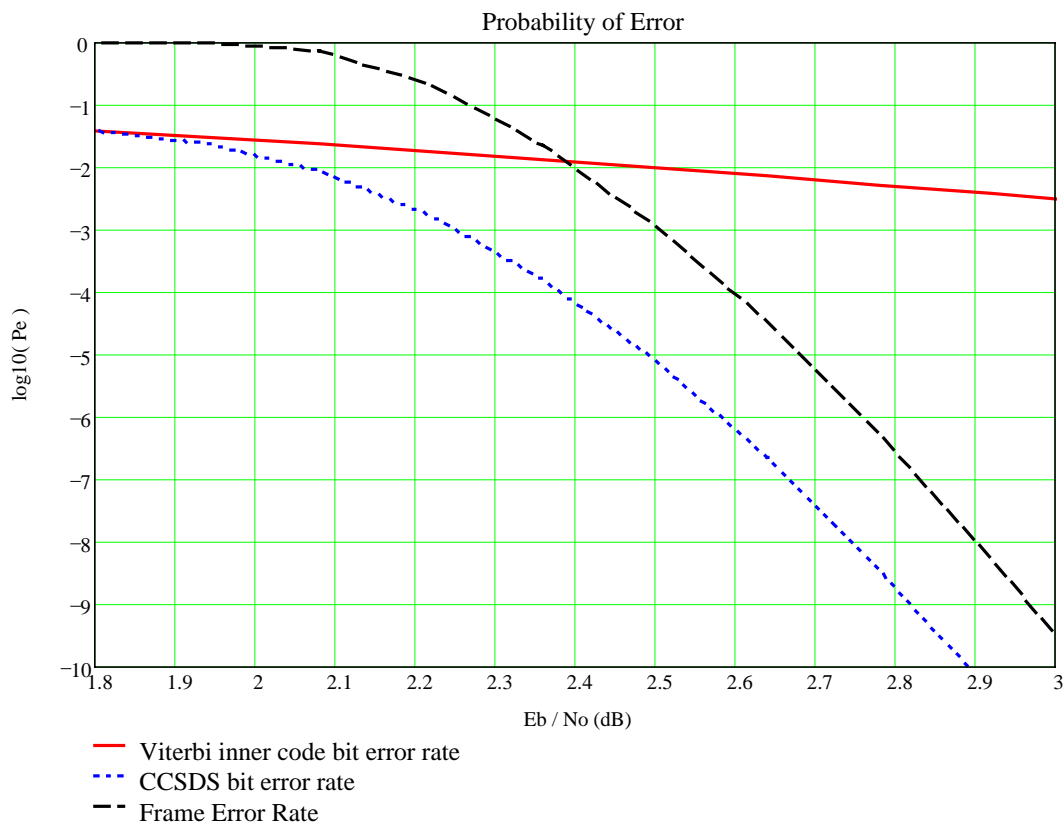


Figure 9: Theoretical E_B/N_O curves.

In the test region of 10^{-1} to 10^{-2} frame failure rate, the E_B/N_O required is approximately 2.3dB (0.4dB below the operating point) and the slope about 0.2dB/decade to 0.1dB/decade. Since our error rate is typically known to about $\pm 20\%$, this is approximately ± 0.08 decades or less than ± 0.016 dB uncertainty, illustrating how the overall accuracy is dominated by the spectrum analyser linearity and signal/noise stability.

The overall budget is illustrated in Table 11 below.

 VES ENGINEERING	Meteosat Second Generation DADF User Station Design Justification Simulators and Test Equipment	 EUMETSAT
VCS/DADF/UST/DSP/016 Issue: 5.0 Date: 1999-08-23		EUM/MSG/SPE/128 Issue: 5.0 Date: 1999-08-23

Table 11: Error Analysis Budget

#	Source	Effect
1	Spectrum analyser accuracy	< 0.1dB leading to < 0.2dB on E_B/N_0
2	Spectrum analyser noise correction	0.01dB
3	Amplitude Stability	0.05dB
4	Signal accuracy	0.01dB
5	Error rate determination	0.016dB
	Total	0.29dB Worst case, Root Sum Square = 0.21dB

One final point is the accurate calibration and testing would be performed on the first "ideal signal" test of the MUBM. Following this the digital pattern could be changed with no significant calibration implications (other than amplitude/time stability) to a pattern with EDA phase & amplitude effects included.

	Meteosat Second Generation	
VCS/DADF/UST/DSP/016 Issue: 5.0 Date: 1999-08-23	DADF User Station Design Justification Glossaries	EUM/MSG/SPE/128 Issue: 5.0 Date: 1999-08-23

8 Glossaries

Please refer to [FGLO].

	Meteosat Second Generation	
VCS/DADF/UST/DSP/016 Issue: 5.0 Date: 1999-08-23	DADF User Station Design Justification Annex A: User Station Data Dictionary	EUM/MSG/SPE/128 Issue: 5.0 Date: 1999-08-23

9 Annex A: User Station Data Dictionary

This section is for compatibility to the USDS only.

	Meteosat Second Generation	
VCS/DADF/UST/DSP/016 Issue: 5.0 Date: 1999-08-23	DADF User Station Design Justification Annex B: PLL Design and Simulation	EUM/MSG/SPE/128 Issue: 5.0 Date: 1999-08-23

10 Annex B: PLL Design and Simulation

	Meteosat Second Generation	
VCS/DADF/UST/DSP/016 Issue: 5.0 Date: 1999-08-23	DADF User Station Design Justification Annex C: Design of Baseband Processing	EUM/MSG/SPE/128 Issue: 5.0 Date: 1999-08-23

11 Annex C: Design of Baseband Processing

	Meteosat Second Generation	
VCS/DADF/UST/DSP/016 Issue: 5.0 Date: 1999-08-23	DADF User Station Design Justification Annex D: Harris HSP50214 Filter Coefficient Table	EUM/MSG/SPE/128 Issue: 5.0 Date: 1999-08-23

12 Annex D: Harris HSP50214 Filter Coefficient Table

	Meteosat Second Generation	
VCS/DADF/UST/DSP/016 Issue: 5.0 Date: 1999-08-23	DADF User Station Design Justification Annex D: Harris HSP50214 Filter Coefficient Table	EUM/MSG/SPE/128 Issue: 5.0 Date: 1999-08-23

	Meteosat Second Generation	
VCS/DADF/UST/DSP/016 Issue: 5.0 Date: 1999-08-23	DADF User Station Design Justification Annex E: MATHCAD Files	EUM/MSG/SPE/128 Issue: 5.0 Date: 1999-08-23

13 Annex E: MATHCAD Files

Annex E of USDJ is a separate Document.